EUROPEAN COMMISSION

nuclear science and technology

Development of Hydro-mechanical Models of the Callovo-Oxfordian Argillites for the Geological Disposal of Radioactive Waste

(MODEX-REP)

Edited by Kun Su
Agence nationale pour la gestion des déchets radioactifs (Andra), FR

Final report

Contract N° FIKW-CT-2000-00029

Work performed as part of the European Atomic Energy Community's R&T specific programme Nuclear Energy 1998-2002, key action Nuclear Fission Safety Area: Safety of the fuel cycle

Directorate-General for Research
2007 Euratom EUR 20844

ACKNOWLEDGEMENTS

This work has been performed by researchers and engineers from the organisations Andra, Coyne et Bellier, ENRESA, GRS, Nagra, SCK/CEN, G3S, LML, ENSMP-CGES-Armine, ITASCA, CIMNE, LAEGO, INERIS, and DBE.

Special thanks are due to the European Commission officer Christophe Davies for his engagement and support of the project in all its phases.

LIST OF PARTICIPANTS

Project co-ordinator

Agence nationale pour la gestion des déchets radioactifs (**Andra**), France – Kun Su, Nasser Hoteit, Gilles Armand, Karim Ben-Slimane and Jean-Domique Barnichon.

Project participants

- Coyne et Bellier (**COB**), France – Anne Bouvard and Eric Boidy;
- Empresa nacional de residuos radiactivos, S.A. (**ENRESA**), Spain – Juan-Carlos Mayor;
- Gesellshaft für Anlagen-und Reaktorsicherheit (**GRS**), Germany – Rothfuchs Tilmann and Chun-Liang Zhang;
- Nationale Genossenshaft für die Lagerung radioactiver Abfälle (**Nagra**), Switzerland – Peter Blumling and Tim Vietor;
- Belgian Nuclear Research Centre (**SCK/CEN**), Belgium – Frédéric Bernier, Xavier Sillen and Xian-Ling Li;
- Groupement d'intérêt public pour l'étude des structures souterraines de stockage (**G3S**), France – Nguyen Minh Duc, Serge Chanchole and Quoc Thai Pham;
- Université des sciences et technologies de Lille, Laboratoire de Mécanique de Lille (**LML**), France – Jian-Fu Shao, Gille Duveau and Yun Jia;
- École nationale supérieure des mines de Paris (**ENSMP-CGES-Armine**), France – Gérard Vouille, Michel Tijani and Ahmed Rouabhi;
- ITASCA Consultants SA, France – Daniel Billaux and Fabien Dedecker;
- Centro internacional de métodos numericos en la enginería (**CIMNE**), Spain – Antonio Gens and Jean Vaunat.

The following laboratories and organisations were invited by Andra to participate in a number of modelling tasks and progress meetings:

- Laboratoire Environnement, géomécanique et ouvrages (**LAEGO**), France – Richard Giot and Albert Giraud;
- Institut national de l'environnement industriel et des risques (**INERIS**), France – Mountaka Souley and Alain Thoraval;
- Deutsche Gesellschaft zum Bau und Betrieb von Endlagern für Abfallstoffe mbH (**DBE**), Germany – Michael Jobmann and Michael Ploster;
- Kungliga tekniska högskolan (**KTH**), Sweden – Ki-Bok Min and Oven Stephansson.

EXECUTIVE SUMMARY

The MODEX-REP project aimed at building and validating suitable constitutive models and numerical tools for the Callovo-Oxfordian argillites investigated by Andra as a potential host rock located at a depth of 500 m in eastern France. Constitutive models are basic tools for assessing the short- and long-term mechanical behaviour of the rock mass in which waste disposal cells are excavated. During the shaft-sinking operations which lasted from 2000 to 2005 at the Meuse/Haute-Marne Underground Research Laboratory (MHM URL) built by Andra, a set of hydro-mechanical instruments recorded the response of the argillites during an in-situ experiment known as the REP experiment.

The MODEX-REP project consisted in:

(i) developing constitutive models by analysing laboratory test results on argillite samples;
(ii) forecasting the response of the rock mass to shaft-sinking operations – the REP experiment;
(iii) analysing the results of in-situ measurements obtained in the REP experiment;
(iv) comparing the forecasted and measured responses of the rock mass; and
(v) validating the models.

For elaborating the constitutive models for the argillites, Andra managed a database of more than 1000 mechanical and thermo-hydro-mechanical coupling tests on argillites samples. Each research team analysed the mechanical and hydro-mechanical behaviour of the rock at sample scale and characterised the main features of the investigated rock: deformability, strength, desiccation effects, creep, swelling and shrinkage. Meanwhile, an important laboratory test programme was carried out by GRS on the argillites samples collected in the REP experiment level from the borehole EST205 that had been drilled in the axis of the auxiliary shaft.

The gas permeability of the rock was measured on wet and saturated specimens, as well as on dried specimens, under confining pressures up to 16 MPa. The effects of desaturation and confining pressure on the gas permeability of the rock were studied. Desaturation increases the gas permeability by three orders of magnitude. The dependency of the gas permeability on the confining pressure is not very significant. Furthermore, in the testing range, the permeability perpendicular to the bedding plane is about one order of magnitude lower than that parallel to the bedding. The creep rate of the argillites was studied under various deviatoric stresses. Long-term single-level creep tests under uniaxial conditions and a low deviator (0.73 to 1 MPa) were also carried out. Results do not confirm the existence of a creep threshold on argillite samples. Creep curves show an almost constant creep rate ($4.4 – 6.7 \bullet 10^{-11}$ s^{-1}) beyond two months. Moreover, results highlighting the dominant effects of dehydration/saturation processes on time-dependent deformation mechanisms in the argillites were obtained.

Based on laboratory test results, both short-term and time-dependent behaviour models of the Callovo-Oxfordian argillites were developed by the MODEX-REP teams. In the case of the short-term behaviour, the following models were proposed for the investigated rock: elastoplastic model with or without softening/hardening, elastoplastic model with damage, discrete model and elastoplastic model with hydro-mechanical-coupling. With regard to the time-dependent behaviour, various methods were used: viscoplastic model, deferred-damage model and deferred-bond failure model. The numerical simulations of laboratory compression tests and creep tests were compared among the research teams. They showed significant discrepancies between creep models, especially due to the scattering of experimental results between samples. Such an

experimental scattering increases uncertainties of the capability of the models to forecast the deferred behaviour of the rock.

In order to test the capability of the numerical codes used for the predictive modelling of the REP experiment, a simplified and typical hydro-mechanical problem was defined, the corresponding semi-analytical solution was established. The problem was then resolved by various numerical codes used in the project. Despite the fact that each team chose a different technique to solve the plastic problem, the overall results agreed. The causes of some discrepancies were identified.

In the framework of the project, predictive modelling (blind prediction) of the REP experiment was carried out in two phases according to two technical specifications prepared by Andra.

- The first modelling, completed in March 2003, was based on the planned excavation method and the REP-experiment design.
- The second predictive modelling campaign was conducted between April and October 2005, based on the *in-situ* real work schedule et the position of sensors.

In general, blind predictions tend to overestimate shaft convergence. Among different results, six teams supplied relatively good forecasts of maximum convergence. In terms of the evolution of convergence over time, Nagra, DBE, LAEGO and CGES-ENSMP provided a relatively good agreement with in-situ results.

The numerical predictions of the pore-pressure evolution at the measurement points are very scattered. SCK/CEN, UPC, LML, LAEGO and G3S teams provided a relatively good agreement with in-situ measurements at some measurement points. G3S considered the desiccation phenomena due to ventilation; the pore pressure in the near-field decreased much more rapidly (numeral results) than the measurements. LML considered permeability changes in the EDZ (elastoplastic with damage model) and results reproduced approximately the pressure evolution in some points. The displacements inside the rock mass supplied by different teams were very scattered. The results supplied by DBE, LML and SCK/CEN were in good agreement for some measurement points. The extension of the very limited fractured zone and of the micro-fractured zone was correctly forecasted by numerical models. From that point of view, the capability of models for predicting the EDZ extension is good in the case of the argillites located in the section of REP experiment.

In-situ measurements recorded during the REP experiment were supplied to all research teams after the blind-prediction modelling. Orientations for improving numerical and constitutive models were discussed by analysing the gaps between numerical and in-situ measurements. Interpretative modelling was then carried out between October 2005 and February 2006. Significant advances were obtained and gaps between interpretative modelling and in-situ measurements were significantly reduced.

The following lessons may be drawn from the project:

- Scale effects on the mechanical strength of the argillites located in the REP section are small due to the high homogeneity of the rock in that zone.
- The short-term constitutive models of the argillites at low and middle deviatoric stress levels need to be improved in order to understand the instantaneous water-pressure drop and pressure distribution in the near-field observed during the REP experiment. The

effect of ventilation on water pressure within the adjacent rock mass requires further investigations.

- The capability to forecast (blind prediction) the hydro-mechanical coupling of the argillites must be improved. The issue about the failure and damage criteria of argillites under effective stress is still pending. It is particularly important for assessing the time-dependent behaviour of the argillites by hydro-mechanical calculations.

In order to share the advancement in constitutive models and numerical modelling realised by the project, a workshop was organised in June 2006 at University Paris XI Orsay. Progress and lessons drawn from the present project, as well as the in-situ measurements of the shaft sinking, are presented. The radioactive waste management organisations, as well as the participants in the present project will integrate the project's results in the simulation of mechanical evolution of disposal cells. In particular, for Andra, the verified hydro-mechanical constitutive models and numerical models stemming from the project will be applied first to refine the design of subsequent underground mechanical experiments in the Meuse/Haute-Marne URL, secondly to supply numerical results for confirming the design of disposal shafts and galleries, and thirdly to demonstrate the performance and safety of disposal in the argillite formation.

For other EU partners (ENRESA, Nagra, GRS, SCK/CEN), improved hydro-mechanical models for the argillite will be compared with the models of their argillaceous rocks. The lessons learnt from the project will lead the partners to re-examine their models and improve the method of development of constitutive models.

TABLE OF CONTENTS

1. INTRODUCTION TO THE MODEX-REP PROJECT

1.1. Objective and organisation

In the European Union, deep argillaceous rock is considered as a potential host rock for the construction of repositories for the disposal of radioactive waste by the following States: Belgium, Spain, Germany, Italy and France. The same choice was made by Switzerland, which is not part of the European Union. The key geomechanical questions raised for such a host formation are similar in those countries: the thermo-hydro-mechanical-coupled constitutive models of the rock, although there are differences in the mineralogical composition of the selected argillaceous formations. Constitutive models represent basic tools for assessing the short- and long-term mechanical behaviour of the rock mass in which waste disposal cells are excavated.

The MODEX-REP project aimed at building and validating suitable constitutive models and numerical tools for the Callovo-Oxfordian argillites investigated by Andra as a potential host rock located at a depth of 500 m in Eastern France. During the shaft-sinking operations at the Meuse/Haute-Marne Underground Research Laboratory (MHM URL) built by Andra, a set of hydro-mechanical instruments recorded the response of the argillaceous rock (called "Callovo-Oxfordian argillites") during an in-situ experiment known as the REP experiment.

The MODEX-REP project, 42 % of which was co-funded by the European Commission as part of the Fifth Euratom Framework Programme (1998-2002), consisted in:

(i) developing constitutive models by analysing laboratory test results on argillite samples;
(ii) forecasting the response of the rock mass to shaft-sinking operations – the REP experiment;
(iii) analysing the results of in-situ measurements obtained in the REP experiment;
(iv) comparing the forecasted and measured responses of the rock mass; and
(v) validating the models.

In order to reach that goal, the MODEX-REP project includes five work packages (WP):

- WP1: Analysis of geomechanical data and development of constitutive models;
- WP2: Study of the capability of constitutive models and numerical tools to deal with hydro-mechanical coupling effects;
- WP3: Predictive modelling of the REP experiment;
- WP4: Comparison between *in-situ* measurement and predictive modelling, interpretive modelling;
- WP5: Lessons learnt from the methodology of the study, as well as the development and validation of constitutive models.

The project was co-ordinated by Andra, under the responsibility of Mr Kun Su.

Eleven European partners were involved in the project:

- Agence nationale pour la gestion des déchets radioactifs (Andra), France;
- Coyne et Bellier (COB), France;
- Empresa nacional de residuos radiactivos, SA (ENRESA);
- Gesellshaft für Anlagen-und Reaktorsicherheit (GRS), Germany;

- Nationale Genossenshaft für die Lagerung radioactiver Abfälle (Nagra);
- Belgian Nuclear Research Centre (SCK/CEN), Belgium;
- Groupement d'intérêt public pour l'étude des structures souterraines de stockage (G3S), France;
- Université des sciences et technologie de Lille (EUDIL), France;
- École nationale supérieure des mines de Paris (ENSMP-CGES-Armine), France;
- ITASCA Consultants SA, France;
- Centro internacional de métodos numericos en la enginería (CIMNE), Spain.

In addition, the following laboratories and organisations were invited by Andra to participate in a number of modelling tasks and progress meetings:

- Laboratoire Environnement, géomécanique et ouvrages (LAEGO), France;
- Institut national de l'environnement industriel et des risques (INERIS), France;
- Deutsche Gesellschaft zum Bau und Betrieb von Endlagern für Abfallstoffe mbH (DBE), Germany;
- Kungliga tekniska högskolan (KTH), Sweden.

When possible, the results supplied by those teams were integrated in this report.

Lastly, Alexis Courtois and Patrick Desgree from EDF France were invited by Andra to participate in several progress meetings.

1.2. Overview of completed tasks

The project started in October 2000 and ended in March 2006. It lasted 30 months longer than expected due to a 24-month moratorium between April 2003 and March 2005, following a delay in shaft-sinking operations caused by two accidents that occurred in the shaft in 2001 and 2002.

In spite of the delay, the entire work covered by the Euratom contract was completed by March 2006. The milestones and the main work performed are summarised below.

1.2.1. Analysing of existing geomechanical data for developing constitutive models (October 2000 to October 2001)

Andra managed a database of more than 1000 mechanical and thermo-hydro-mechanical coupling tests on samples. Each research team analysed the mechanical and hydro-mechanical behaviour of the rock at sample scale and characterised the main features of the investigated rock: deformability, strength, desiccation effects, creep, swelling and shrinkage. Moreover, the Geological Statement Report prepared by Andra in 1999, in which the mechanical behaviour of the rock was summarised, was translated into English and sent to all research teams. That document consists of a key input report about the geology, geomechanics and hydrogeology of the investigated formation.

1.2.2. Laboratory testing on argillite samples collected from the REP experiment zone (October 2000 to June 2002)

A laboratory test plan was proposed by GRS and discussed with Andra. Andra sent GRS seven core samples (300 by 110 mm) of the Callovo-Oxfordian argillites collected from borehole EST205 that had been drilled in the axis of the auxiliary shaft. Those original samples were divided into 28 argillite samples for the purposes of eleven creep tests, eight permeability tests, seven relaxation tests and six compression tests [2].

The gas permeability of the rock was measured on wet and saturated specimens, as well as on dried specimens, under confining pressures up to 16 MPa. The effects of desaturation and confining pressure on the gas permeability of the rock were studied. Desaturation increases the gas permeability by three orders of magnitude. The dependency of the gas permeability on the confining pressure is not very significant. Furthermore, in the testing range, the permeability perpendicular to the bedding plane is about one order of magnitude lower than that parallel to the bedding.

The creep rate of the argillites was studied under various deviatoric stresses. Long-term single-level creep tests under uniaxial conditions and a low deviator (0.73 to 1 MPa) were also carried out. Results do not confirm the existence of a creep threshold on samples. Creep curves show an almost constant creep rate ($4.4 – 6.7 \cdot 10^{-11}$ s^{-1}) beyond two months.

During the last phase of a creep test under an axial stress of 15 MPa, two specimens were exposed to ambient air with a relative humidity of 24.0 ± 3.4 % in order to examine moisture effects on the time-dependent behaviour. It was shown that, over 40 days, under a stress of 15 MPa, the air-dried specimens deformed steadily backwards with negative rates of $– 10^{-11}$ per second (swelling). Such a result highlights the dominant effects of dehydration/ saturation processes on time-dependent deformation mechanisms in the argillites.

In addition, the results of creep tests over three years conducted by G3S in the framework of a direct contract with Andra were supplied to all research teams in 2002 in order to develop the time-dependent behaviour model of the argillites.

1.2.3. Testing the capability of numerical codes to simulate an excavation with hydro-mechanical coupling (October 2000 to June 2001)

In order to test the capability of the numerical codes used for the predictive modelling of the REP experiment, CGES and Andra defined a simplified and typical hydro-mechanical problem and established a semi-analytical solution. The problem was then resolved by various numerical codes. The numerical codes used in the exercise included: VIPLEF Code of CGES-ENSMP; CASTEM2000 used by G3S; MPPSAT Codes of LML; CODE_BRIGHT of CIMNE, and PFC Code of ITASCA France. The CYSIF Code developed by *École des mines de Paris* in 1976 was used to provide the semi-analytical solution of the problem.

Despite the fact that each team chose a different technique to solve the plastic problem (variable or constant stiffness matrix) and a different method to simulate hydro-mechanical coupling (full coupling or external iterative process), the overall results agreed. Discrepancies were observed for two codes: the PFC Code used by ITASCA and the CASTEM2000 Code used by G3S. The causes of those discrepancies were identified.

1.2.4. Development of constitutive models by different partners (October 2000 to June 2002)

Based on laboratory test results, both short-term and time-dependent behaviour models of the Callovo-Oxfordian argillites were developed by the MODEX-REP teams and were discussed during the second and third progress meetings.
In the case of the short-term behaviour, the following models were proposed for the investigated rock: elastoplastic model with or without softening/hardening, elastoplastic model with damage, discrete model and elastoplastic model with hydro-mechanical-coupling. With regard to the time-dependent behaviour, various methods were used: viscoplastic model, deferred-damage model and deferred-bond failure model. The numerical simulations of laboratory compression tests and creep tests were compared among the research teams. They showed significant discrepancies between creep models, especially due to the scattering of experimental results between samples. Such an experimental scattering increases uncertainties of the capability of the models to forecast the deferred behaviour of the rock. A creep-test curve may be easily well fitted, but it is very difficult for it to fit well simultaneously several creep tests using the same set of parameters [3].

1.2.5. Specifications for shaft-sinking modelling (January to December 2002 and March to June 2005)

Andra prepared two specifications, in 2002 and 2005, respectively, with a view to simulating the REP experiment [4] [5]. The geometry of the argillite formation, the shaft design, the support and lining method and the mechanical characteristics of the lining material, the excavation method, the proposed schedule for excavation and the advancement of the concrete lining, the type and position of implemented sensors in the adjacent rock mass, as well as the expected numerical results are specified. Based on those documents, numerical models were drawn.

1.2.6. Predictive modelling of the REP experiment and comparison with the *in-situ* experiment (December 2002 to March 2003 and April 2005 to October 2005)

In the framework of the MODEX-REP project, predictive models (blind prediction) of the REP experiment were built in two phases:

- the first step, completed in March 2003, was based on the planned excavation method and the REP-experiment design. Nine research teams presented their numerical approaches to simulate the mechanical and hydro-mechanical response of the argillites to shaft-sinking operations (4th progress meeting, 27 February 2003). Three of the teams (Andra, SCK/CEN and Nagra) used 3-D models, while the others proposed 2-D plane or 2-D axisymmetric models. In 3-D models, shaft-sinking operations are simulated step by step by adding or deleting mesh or modifying the mechanical characteristics of the relative volume of muck. In 2-D models, shaft-sinking activities are simulated by unloading progressively stresses and pore pressures on the shaft wall. Shaft displacement and the extension of the plastic zone are compared between the models;

- the second predictive modelling campaign (blind prediction) was conducted by 10 research teams between April and October 2005. Seven numerical codes were used: VIPLEF, ABAQUS, FLAC3-D, PFC2-D, Code_Aster, THMPASA, Code_Bright. The constitutive models being used were those developed in the framework of the MODEX-

REP project. A comparison with *in-situ* measurements was made during the sixth progress meeting held on 17 October 2005.

In general, numerical models tend to overestimate shaft convergence. Among different results, six teams supplied relatively good forecasts of maximum convergence. In terms of the evolution of convergence over time, Nagra, DBE, LAEGO and CGES-ENSMP provided a relatively good agreement with *in-situ* results.

The numerical results of the pore-pressure evolution at the measurement points are very scattered. SCK/CEN, UPC, LML, LAEGO and G3S teams provided a relatively good agreement with *in-situ* measurements at some measurement points. G3S considered the desiccation phenomena due to ventilation; the pore pressure in the near-field decreased much more rapidly (numeral results) than the measurements. LML considered permeability changes in the EDZ (elastoplastic with damage model) and results reproduced approximately the pressure evolution in some points. The displacements inside the rock mass supplied by different teams were very scattered. The results supplied by DBE, LML and SCK/CEN were in good agreement for some measurement points.

1.2.7. Interpretative modelling of REP experiment and analysing discrepancies between numerical models and *in-situ* observations (October 2005 to February 2006)

In-situ measurements recorded during the REP experiment were supplied to all research teams after the blind-prediction modelling. Andra presented and analysed the results during the 6th progress meeting held on 17 October 2005. Orientations for improving numerical and constitutive models were discussed by analysing the gaps between numerical and *in-situ* measurements. Moreover, in order to make future comparisons, the confidence in the precision of *in-situ* measurement was graded according to the analysis of all parameters involved in the instrumentation set-up.

Interpretative modelling was then carried out between October 2005 and February 2006. Numerical results from nine teams were compared once again with *in-situ* results at the seventh progress meeting held on 22 February 2006. Significant advances were obtained and gaps between numerical and *in-situ* measurements were significantly reduced.

1.2.8. Lessons learnt

The following lessons may be drawn from the project:

- scale effects on the mechanical strength of the argillites located in the REP section are small due to the high homogeneity of the rock in that zone;
- the short-term constitutive models of the argillites at low and middle deviatoric stress levels need to be improved in order to understand the instantaneous water-pressure drop and pressure distribution in the near-field observed during the REP experiment. The effect of ventilation on water pressure within the adjacent rock mass requires further investigations;
- the capability to forecast (blind prediction) the hydro-mechanical coupling of the argillites must be improved. The issue about the failure and damage criteria of argillites under effective stress is still pending. It is particularly important for assessing the time-dependent behaviour of the argillites by hydro-mechanical calculations.

In conclusion, the MODEX-REP project has shown that the blind prediction of the *in-situ* experiment remains an efficient means to assess the capability of numerical models and constitutive laws to simulate the evolution of underground structures over time.

2. ANALYSIS OF ARGILLITES HYDRO-MECHANICAL BEHAVIOUR OBSERVED ON SAMPLES

In order to develop constitutive models for mechanical and hydro-mechanical behaviour, the Callovo-Oxfordian argillites were submitted to characterisation studies during their saturated and unsaturated states since 1996. At the beginning of the MODEX-REP project, Andra managed a database containing more than 1,000 mechanical and thermo-hydro-mechanical coupling tests on argillite samples. Each research team analysed the mechanical and hydro-mechanical behaviour, and determined the main features of the investigated rock: deformability, strength, desaturation effects, creep rate, swelling and shrinkage. Moreover the laboratory test results obtained by GRS in the framework of the MODEX-REP project were made available to all partners.

The following sections summarise the hydro-mechanical behaviour observed on argillite samples, with a special focus on the results achieved by the MODEX-REP project. A comparison is first made of three argillaceous rocks being investigated in Europe.

2.1. Basic properties of three clays currently studied in Europe

In Europe, there are three clay formations that are currently studied in detail as potential host rocks for the implementation of a repository for high-level and long-lived radioactive waste: Boom clay in Belgium, Opalinus clay in Switzerland and Callovo-Oxfordian clay in France. Those formations represent a spectrum ranging from clay with 40 % volumetric water content with relatively high plasticity up to a highly consolidated stiff clay stone with volumetric water content as low as 5 %.

2.1.1. Boom clay

Boom Clay consists of marine fine-grained sediment of the Rupelian Age. It shows a characteristic layering, which is the result of variations in grain sizes, organic matters and carbonates. The granulometry indicates a relatively wide variation; the clay fraction (< 2μm) ranges from 30 to 70 % (average of 55 %). The clay mineralogy is dominated by illite (50 %), smectite and illite-smectite interstratifications (30 %), kaolinite (10 %), chlorite (5 %), degraded chlorite and illite-chlorite interlayers, as well as glauconite (3 %). Muscovite and biotite (mica minerals) are only present in small quantity. Boom clay also contains 1-5 % of carbonates, pyrite and organic matter. Its hydro-mechanical properties are commonly considered as homogeneous. The basic geomechanical characteristics and conditions of Boom clay around the Mol Underground Laboratory (225 m in depth) are presented in Table 1. The hydraulic conductivity of Boom clay in the flow direction parallel to the bedding plane is twice that of the orthogonal direction to the bedding plane.

2.1.2. Opalinus clay

Opalinus clay generally consists of dark grey, silty, calcareous and micaceous clay stones of the Jurassic Age. In the Zürcher Weinland, Northern Switzerland, the Murchisonae Beds (approximately 20 m thick) located above the Opalinus clay consist of black silty to fine sandy, calcareous claystones and are thus similar, in terms of lithology, to the uppermost Opalinus clay.

Mineralogical investigations show that the phyllosilicate fraction contains mainly kaolinite, illite and illite/smectite interlayer minerals in about equal amounts (average amount 54 % at Benken) [6]. The carbonate content is rather high ranging from 10 to 50 % (average 26 % at Benken), and dominated by calcite. Quartz is also present in relatively large quantities (average 20 % at Benken). The content of organic matter is about 0.5 %.

The mechanical properties of Opalinus clay were found to be highly anisotropic (transversally isotropic). A dependency of the elastic properties and strength parameters on water content are observed. In addition, a transition was noticed from brittle behaviour at lower water contents to more ductile behaviour at high water content. The physical properties of the rock depend to a lesser extent on its mineral composition. Although no direction dependency was observed for Poisson's ratio, the elasticity moduli show a clear anisotropy in relation to stratification with $E_{parallel} > E_{45°} > E_{perpendicular}$. The following observations were made in the Zürcher Weinland at a depth of about 600 m (see Table 2).

Table 1. Geomechanical characteristics of Boom clay on the Mol Site, Belgium

Initial total stress	4.5 MPa	Porosity n	0.39
Initial pore pressure	2.25 MPa	Water bulk modulus K_w	0.2-2 GPa
Young's modulus E'	300 MPa	Hydraulic conductivity k	$2 \cdot 10^{-12}$ m/s – $4 \cdot 10^{-12}$ m/s
Poisson's coefficient ν'	0.125	Plastic limit	23-29 %
Cohesion c'	300 kPa	Liquid limit	55-80 %
Friction angle ϕ	18°	Plasticity index	32-51 %
Rc	2 MPa	Water content	22-27 %

Table 2. Geomechanical characteristics of Opalinus clay [6]

Site	**Mont Terri**		**Zürcher Weinland**	
	Matrix	Bedding	Matrix	Bedding
Initial vertical stress	6-7 MPa		15.9 MPa	
Initial max./min. horizontal stress	2-3 MPa/4-5 MPa		22.6-15.1 MPa	
Initial total mean stress	4-5 MPa		18 MPa	
Initial pore pressure	1-2 MPa		6-7 MPa	
Porosity	0.16		0.12	
Young's modulus	6 GPa	3 GPa	10.5 GPa	5 GPa
Poisson's ratio	0.24	0.24	0.27	0.25
Cohesion	3 MPa	1 MPa	6.9-8.6 MPa	1.5-1.7 MPa
Friction angle	25°	23°	21-25°	20-24°
Uniaxial compressive strength	10-16 MPa	No data	30 MPa	6 MPa
Tensile strength	1 MPa	0.5 MPa	2.7 MPa	1.2 MPa
Hydraulic conductivity	8×10^{-14} m/s	2×10^{-13} m/s	2×10^{-14} m/s	1×10^{-13} m/s

2.1.3. Callovo-Oxfordian argillites

Callovo-Oxfordian argillites are marine sediments of the Jurassic Age (about 150 million years old). They are overlain and underlain by relatively impermeable carbonate formations.

The argillites contain an average of 40-45 % clay minerals (illite, regular mixed layer R1 illite-smectite, chlorite and kaolinite in the lower part, illite and irregular mixed layer R0 illite-smectite in the upper part), 20-30 % carbonate and 20-30 % quartz silts. The layer is almost horizontal.

The mechanical behaviour of the rock is ruled by the geological characteristics of the argillites. Its mineralogical composition and sedimentation have led to a slightly anisotropic behaviour of the argillites. The combined effect of sedimentation, compaction and diagenesis has reduced the interstitial or connected pore space. Hence, Callovo-Oxfordian argillites are considered in their natural state as a saturated porous medium with very low permeability. Their mechanical behaviour is closely coupled with the pore pressure and the degree of saturation.

From a geomechanical standpoint, the Callovo-Oxfordian formation may be subdivided into three rheological zones with different geomechanical properties: two stiff (higher carbonate) zones surround a central less stiff (more clayey) zone. Table 3 shows the basic mechanical characteristics of those three zones as observed at a depth varying between 420 and 550 m.

The initial permeability of the intact rock is about 5×10^{-20} m^2 in the direction parallel to the bedding plane, and 5×10^{-21} m^2 perpendicular to the bedding (Andra 2005).

Table 3. Basic mechanical characteristics of the different geological zones of the Callovo-Oxfordian formation (Andra, 2005)

Characteristic	Rheological zone			Overall
	Upper	Median	Lower	
Depth (m)	420-455	455-515	515-550	420-550
Initial total stresses	12-16 MPa at - 500 m			
Initial pore pressure	~ 5 MPa at - 500m			
Density (g/cm^3)	2.42	2.42	2.46	2.40-2.45
Water content (% mass)	6.1	7.1	5.9	5.3-8.0
Porosity (%)	14	15,5	13	11.5-17.0
Young's modulus (GPa)	6.2	5.5	7.2	6.0
Uniaxial compressive strength (MPa)	30	21	21	24
Uniaxial tensile strength (MPa)				2.6
Hydraulic conductivity (m/s)	10^{-13}-10^{-14}			10^{-13}-10^{-14}

2.1.4. Relation between physical parameters and mechanical behaviour

The relationship between the physical parameters and the mechanical behaviour of the argillaceous rocks being studied in France and in Europe was investigated [7]. It showed that the mechanical behaviour of clayey rock is very much influenced by the water content of the material, the burial history and the associated compaction and the anisotropy of the material due to bedding.

In many cases, the history of the stress path of deep sedimentary rocks may be summarised by a normal sedimentation process without any significant impact due to erosion phases. Consequently, according to that simplified scheme, the history of the stress path may be well represented by the burial depth (i.e. by the present *in-situ* mean effective stress). Moreover, it is often observed that dry density rises with increasingly higher carbonate content and decreasing clay content. Hence, dry density or water content may be considered as a representative

parameter, which may explain the main features of the mechanical behaviour of argillaceous rocks.

Figure 1 shows the correlation between uniaxial compressive strengths and dry density. Two domains may be defined with a boundary dry density value ranging from 2.15 to 2.35 g/cm^3. Very steep slopes for the higher dry-density values indicate that a small change in dry density may explain a large variation in the mechanical properties of argillaceous rocks. High density involves a brittle and ductile-brittle behaviour of the rock, whereas lower density represents a ductile behaviour. Figure 2 provides an overview of the uniaxial strength of different clay materials as a function of water content [3].

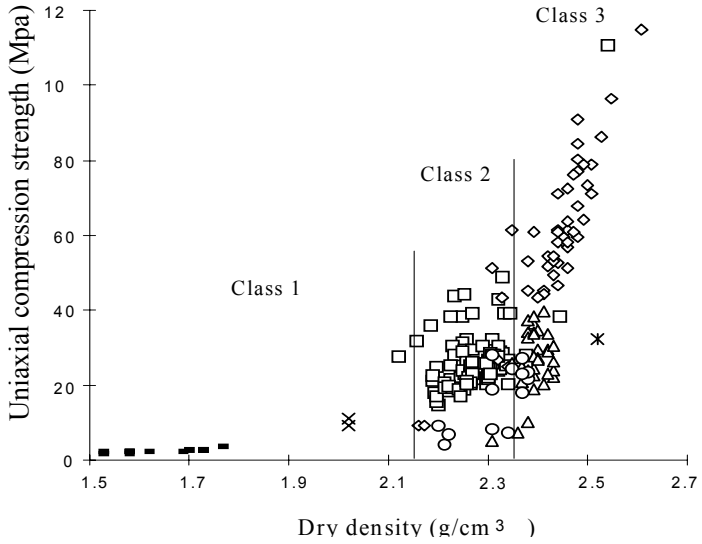

Figure 1. Uniaxial compression strength versus dry density for seven European argillaceous rocks [7]

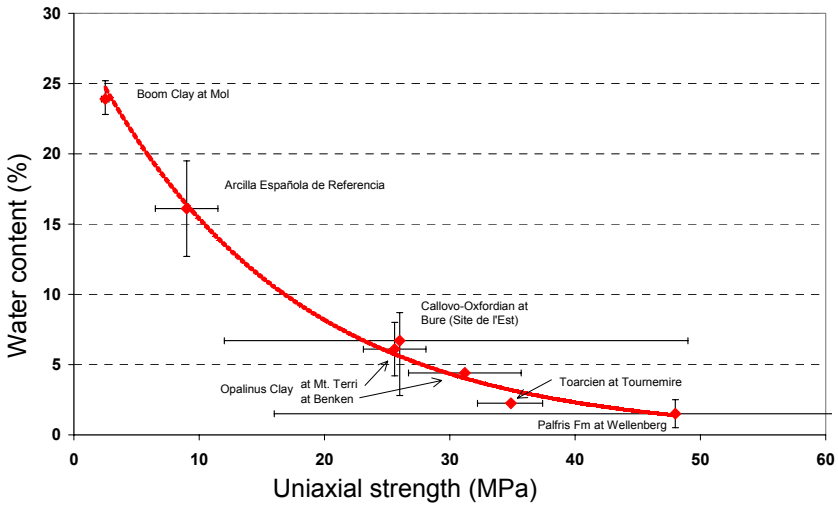

Figure 2. Cross-plot of uniaxial compressive strength and water content for different clays [3]

2.2. Analysis of stress-strain curve of Callovo-Oxfordian argillites

Figure 3 presents typical stress-deformation curves resulting from compression tests at different confining pressures. The tests were carried out with neither resaturation nor interstitial pressure imposed. As a result, these tests are considered to be undrained. A detailed analysis of the mechanical behaviour of argillite samples is given below.

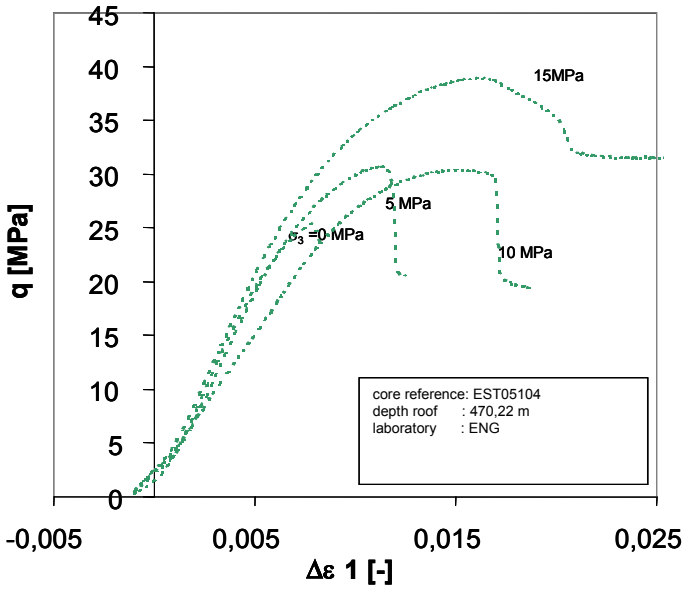

(a) Results obtained by LAEGO [3]

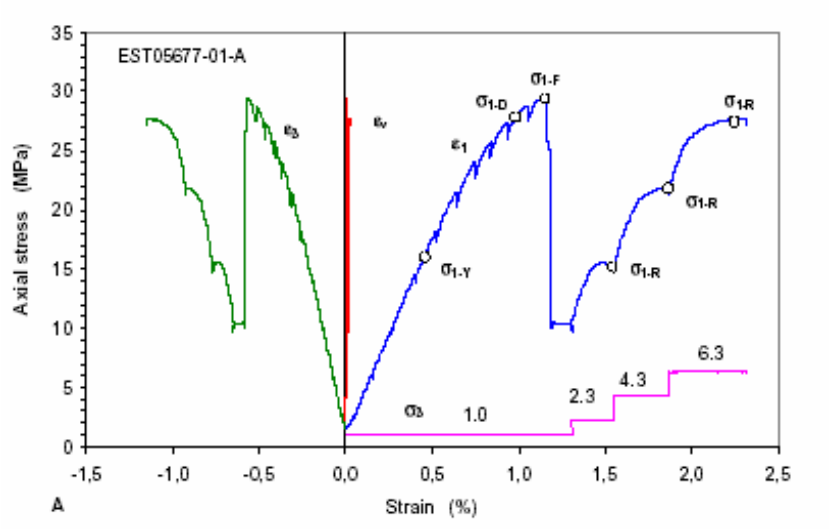

(b) Results obtained by GRS [2]

Figure 3. Typical experimental curves at different confining pressures

Under a **low deviatoric stress**, the response of the argillites is quite linear (stress-deformation relationship), while the deviatoric-stress level remains approximately 50 % below the strength to rupture.

The linearity of the stress-deformation curve simply proves the existence of a constant proportionality between stress and deformation, but is not synonymous as such with a reversible linear elastic behaviour. The unloadings made during that phase show the occurrence of an irreversible contracting deformation under triaxial compression.

Under a **high deviatoric stress**, the loss of linearity noted on the axial stress-deformation and lateral stress-deformation curves appears when the stress level exceeds a threshold of approximately 50 % of the stress to rupture under compression. That stress threshold, which separates the linear and non-linear macroscopic behaviours, marks: (i) the end of free sliding between grains; (ii) the beginning of "inhibited" sliding, and (iii) the beginning and stable propagation of the microfissuring.

Based on microscopic observations made on the samples before and after the mechanical test, a damage scenario without taking into consideration the hydro-mechanical coupling showing the influence of the mineralogical composition may be proposed [8]. Anisotropic damage appears in the form of cleavages in the calcite grains and microfissures, which are created and propagated to the interface between the calcite and quartz grains and the matrix, and then in the matrix itself, following a preferential direction (mainly parallel to the main axial major stress).

The **unstable propagation threshold** of the fissures in the argillites is approximately 90 % of the resistance. The deformations in the test sample become highly heterogeneous and are localised along the shearing strips. The localisation threshold constitutes the real point of initiation of the rupture. On the volumetric stress-deformation curves, the unstable propagation of the fissures is identified by an acceleration of the expanding deformations. The volume of the sample increases, essentially because of the expansion of the shearing strip. The rupture of the argillites under compression and in extension is rather brittle. The increase in the confinement pressure during compression tests confers progressively a ductile behaviour to the argillites. At a confinement pressure of 20 MPa, the behaviour of the argillites becomes practically ductile.

A reduction of the deformation modulus is observed even in the linear part of the stress-deformation curves. The modulus is divided by a factor of 2 to 3 when the deviatoric stress approaches the resistance level of the rock.

The entire **post-peak field** corresponds to the development of the damage in the localised deformation zone leading to the conventional rupture plane in shearing and to the transversal rupture plane, during the triaxial test and the axial-extension test, respectively.

During the residual phase, the development of the rupture under compression results in: (i) the collapse of the sample under non-confined conditions; ii) an almost constant residual resistance, corresponding to the resistance to shearing in the sliding planes under confined conditions, and (iii) the proportional increase of the residual strength with the confining pressure (Figure *3*).

2.3. Deformability of the argillites

Although the definition of the deformation modulus is simple, its determination on argillite samples is delicate due to the non-linearity, natural dispersion and various deformation-measurement methods (overall, local).

Under uniaxial-compression conditions, the variation profile of the tangent modulus, E_t in relation to depth shows a large natural dispersion. The upper part of the layer is characterised by

a tangent modulus E_t and a secant modulus E_s of about 4 900 MPa and 6 200 MPa, respectively, but with a large dispersion (δ/m ~45 %). The more homogeneous and more clayey central part (where the REP experiment took place) with a slightly less important dispersion (20-30 %) has a modulus E_t and E_s of ~ 4 400 MPa 5600, respectively (Andra, 2005).

2.4. Desiccation effects

Desiccation changes significantly the elastic behaviour of the argillites, as shown in

Figure 4, with stress-strain curves of three triaxial tests with different levels of water content as measured after cure. The more the rock sample is desaturated, the deeper is the slope of stress-strain curves in axial and transversal directions. Young's modulus is multiplied by 1.5 between an almost completely saturated sample (w = 7.55 %) and a sample with about 4.6 % water content. Meanwhile, the strength of the rock increases also when the saturation degree decreases.

A set of uniaxial compression tests carried out on the samples that were submitted to a cure with various relative humidity levels before testing show that Young's modulus increases from 2~5 GPa to 10~25 GPa, when relative humidity decreases from 90-100 % to 50 %. The results recorded on other clayey rocks [10] confirm also that Young's modulus of argillaceous rock is multiplied by 3 to 4 when the rock is desaturated. In addition, we note that Young's modulus starts to decrease when the samples are severely desaturated (saturation near 30~0 %).

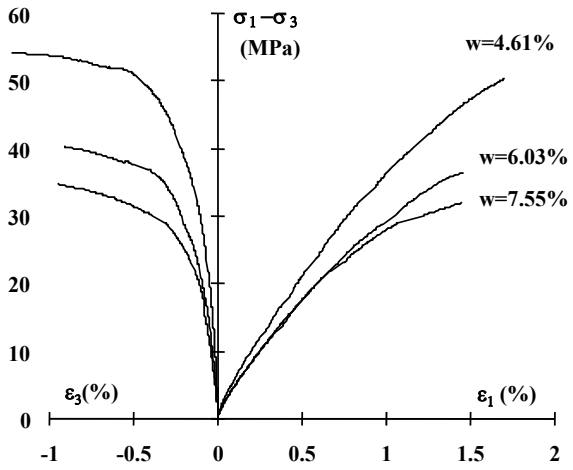

Figure 4. Triaxial tests on argillite samples with different water contents under a 10-MPa confining pressure [8]

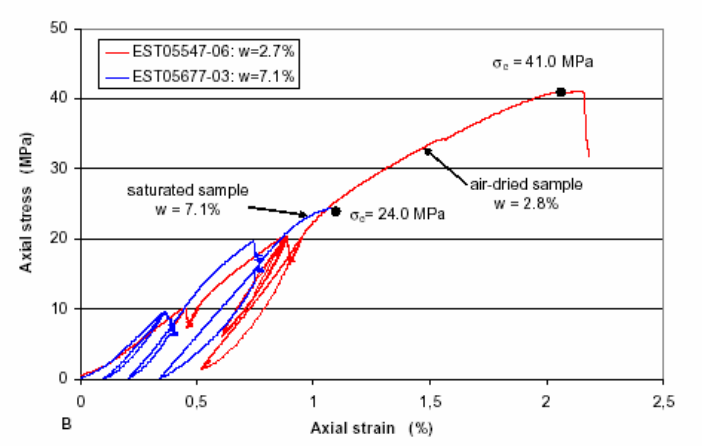

Figure 5. Results of uniaxial compression tests on specimens of Callovo-Oxfordian argillite for two saturation states [2]

2.5. Time-dependent behaviour

Successive creep tests were carried out on argillite samples between 1996 and 2004. Tests results show that the argillites express a time-dependent behaviour even under undrained conditions. That observation confirms that the time-dependent behaviour of the argillites depends both on the viscoplasticity of the material and on compaction phenomena.

The amplitude of the deferred deformations during creep tests is weak. The creep rate under undrained triaxial conditions is about 10^{-6} to 10^{-7}/h (~ 0.1 to 1 %) depending on the loading velocity and the calculation mode of those rates. The comparison between axial and lateral deferred deformations leads to neglect volumetric deformations. The anisotropy of the deferred strains parallel and perpendicular to the stratification is negligible [2]. The strain rate of the sample is independent of its size, which may mean that the scale effects of the rock under study may not be significant on its time-dependent behaviour.

As shown in Figure 6, the deferred strain increases proportionally to the deviatoric stress. The deferred strain remains measurable whatever the deviatoric-stress level. It has been impossible until now to determine a threshold of deviatoric stress below which there would be no deferred strain. With regard to the influence of temperature, it is shown that the time-dependent behaviour may be enhanced by a temperature increase (Figure 6).

In the last creep phase of a creep test at 15 MPa, two specimens were exposed to the ambient air with a relative humidity of 24.0 ± 3.4 % in order to examine the effect of moisture on the time-dependent behaviour, as shown in Figure 7. Since a direct measurement of the desaturation of the creeping specimens was impossible, an accompanying measurement of water-content change on the reference specimen was conducted under the same conditions as in the creep tests. Since the specimens rapidly underwent desaturation during the first few days, the deformations responded simultaneously with a large magnitude of about 0.3 % shrinkage, irrespective of the loading direction. The fluctuations in deformation corresponded to the fluctuations in moisture. Once the specimens were sealed against ambient air conditions, fluctuations in deformation remained minimal. Over the last 40 days, under a stress of 15 MPa, the air-dried specimens deformed steadily backwards with negative rates of -10^{-11}/s (swelling).

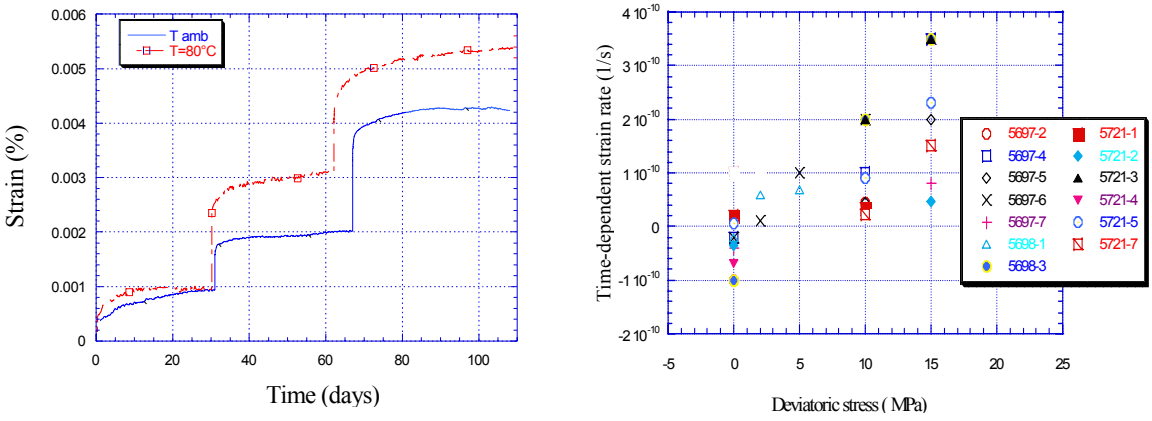

(6a) (6b)

Figure 6 Creep tests on the argillites. 6(a) Effects of temperature and deviatoric stress; 6(b) Strain rate versus deviatoric stress [9]

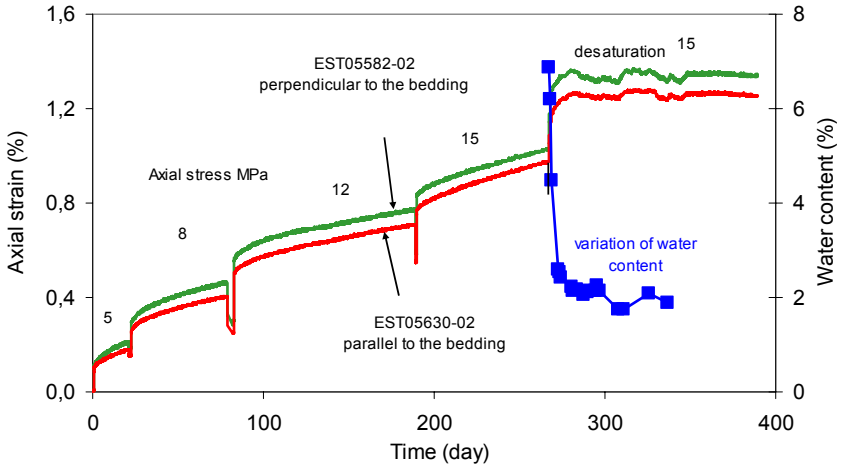

Figure 7. Creep tests on the samples parallel and perpendicular to the stratification and study of desiccation effects on the last loading step [2]

2.6. Hydro-mechanical coupling

The term "hydro-mechanical coupling" designates the interaction between interstitial pressure and mechanical behaviour. In the laboratory, two coupled hydro-mechanical effects were observed on argillite samples: (i) the pore pressure increased during mechanical tests, and (ii) the constancy of the value of the deviatoric stress to rupture under various constant effective confinements (variable total confinement). However, it should be noted that, although the effects of hydro-mechanical coupling may be observed qualitatively on laboratory samples, their quantification remains nonetheless uncertain, since a direct measurement of the pore pressure at the centre of a test sample (a few centimetres in diameter) is not technically feasible.

Two experimental protocols were developed in order to determine the parameters for the hydro-mechanical coupling of argillites (Biot's coefficient, *b,* and Biot's modulus, *M*): the oedometric-cell method and the triaxial-cell method.

The mean value of *b* provided by those methods is 0.60 with a standard deviation of 0.20 for the argillite samples located in the middle of the Callovo-Oxfordian layer. The values of Biot's modulus, *M,* as determined on the samples, vary considerably depending on the experimental method being used and range from 470 to 10 600 MPa. The extremely low values of *M* as determined on samples are probably due to a low desaturation of the samples or the presence of trapped gases in the pores despite the resaturation phase, since air is very highly compressible.

Based on some theoretical relationships between coupling parameters, the possible variations of modulus, *M,* for argillites was studied. For undrained Young's moduli ranging from 4 000 to 6 000 MPa, Biot's modulus, *M,* varies between 4 300 and 8 300 MPa. In addition, the variations of coefficients *b* and *M* are restricted by several inequalities; for instance, the undrained Poisson's coefficient must be greater than 0 ($\nu_0 > 0$).

3. CAPABILITY TEST FOR NUMERICAL CODES

In order to test the capability of the numerical codes being used for the predictive modelling of the REP experiment, CGES and Andra defined a simplified and typical hydro-mechanical problem. The problem was then resolved semi-analytically by CGES and by the various numerical codes used by the research teams.

3.1. Definition of the problem to be resolved

Starting from time $t = 0$, a cylindrical hole (tunnel or shaft) was created in an infinite poro-elastoplastic medium initially subjected to a uniform isotropic state of stress with a uniform pore-pressure field. The evolution of that system at time > 0 was investigated during and after excavation. The gravity forces were neglected.

Hypothesis

* Hydromechanical coupling:
  – Effective stress: $\underline{\sigma_t} = \underline{\sigma} - bp\underline{1}$
* Mechanical behaviour of the material:
  – Failure criterion and potential function – Hoek-Brown:

$$F(\underline{\sigma}, \xi) = \frac{(\sigma_3 - \sigma_1)^2}{R_c} + m\sigma_3 - R_c f(\xi) \leq 0$$

  – Softening effect: $0 < \xi < \xi_R \quad f(\xi) = \left[1 - (1-\alpha)\frac{\xi}{\xi_R}\right]^2$

$$\xi > \xi_R \qquad f(\xi) = \alpha^2$$

$\xi = -\varepsilon_1^p$ where ε_i^p are the principal plastic strains

Initial and boundary conditions of the semi-analytical solution

Hydraulic parameters		**Mechanical parameters**	
Permeability	$k = 10^{-12}$ m/s	Young modulus	E = 5800 MPa
Specific weight of water	$\gamma = 0.01$ MN/m^3	Poisson's ratio	$\nu = 0.3$
Biot coefficient	$b = 0.8$		
Biot modulus	$M = 6000$ MPa		
Hoek and Brown parameters		**Softening parameters**	
$R_c = 14.8$ MPa (uniaxial compressive effective strength)		$\alpha = 0.01$	
$m = 2.62$		$\xi_R = 0.015$	
Geometrical conditions		**Initial conditions (time $t = 0$)**	
Internal radius a = 3 m and external radius b = 30 m		Effective stresses $\underline{Q}$ = 7.74 MPa. Pore pressure 4.7 MPa	

Boundary conditions (time t > 0)

Outer radius (r = b) Constant radial effective stress σ_r = -7.74 MPa

Constant pore pressure p = 4.7 MPa

Inner radius (r = a) For $0<t<T$ $\sigma_r = -7.74(1-t/T)$ in MPa T = 1.5 Ms

$p = 4.7(1- t/T)$ in MPa, $t>T$ $\sigma_r = p = 0$

Semi-analytical solution

Developed at the *École des mines de Paris* in 1976, the CYSIF Code is used to solve problems relating to cylindrical and spherical holes in homogeneous infinite media (1-D problems). Mechanical equations are transformed analytically by reducing them to simple integrals, which may be approached numerically by a simple trapezoidal technique. Such a code, when used for a linear problem (elasticity), provides the exact solution (closed-form solution).

In the case of coupling phenomena (thermo-hydro-mechanical problems), thermal and hydraulic problems are solved by an external 1-D classical finite-element code, while an external iterative process is used to fulfil the coupling

The response of the material under triaxial test conditions is plotted in Figure 8.

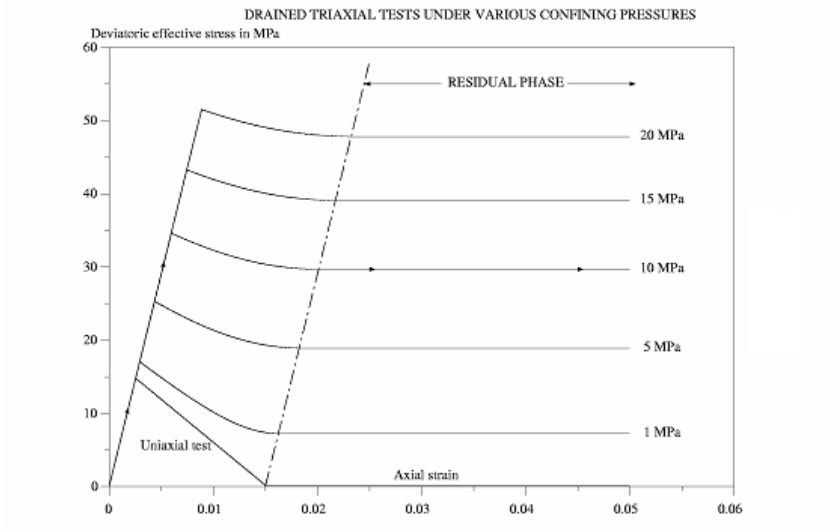

Figure 8. Simulation of triaxial compression tests using the poro-elastoplastic model defined in the benchmark test

3.2. Comparison results

The numerical codes used in the exercise included: the VIPLEF Code of CGES-ENSMP, the CASTEM2000-G3S Code, the MPPSAT codes of LML, CODE_BRIGHT of CIMNE and the PFC Code of ITASCA France.

Figure 9, Figure 10, and Figure 11 show a comparison between the semi-analytical solution and the numerical results. Discrepancies were observed for two codes: the PFC code used by ITASCA and the CASTEM2000 Code used by G3S. Those discrepancies may be explained as follows:

(i) the PFC Code is based on the principle of a discrete model; the input rheological parameters for solving the problem are calibrated on numerical compression tests supplied by CGES and some uncertainty (10~15 %) may subsist in the calibration of model parameters;

(ii) the CASTEM2000 Code does not include the Hoek-Brown criterion on hydro-mechanical coupling and G3S uses the equivalent Drucker-Prager criterion to solve the problem; in the current case, plastic strains induced by the equivalent model are different from the original criterion.

Despite the fact that each team chose a different technique to solve the plastic problem (variable or constant stiffness matrix) and a different method to simulate the hydro-mechanical coupling (full coupling or external iterative process), the overall results agreed.

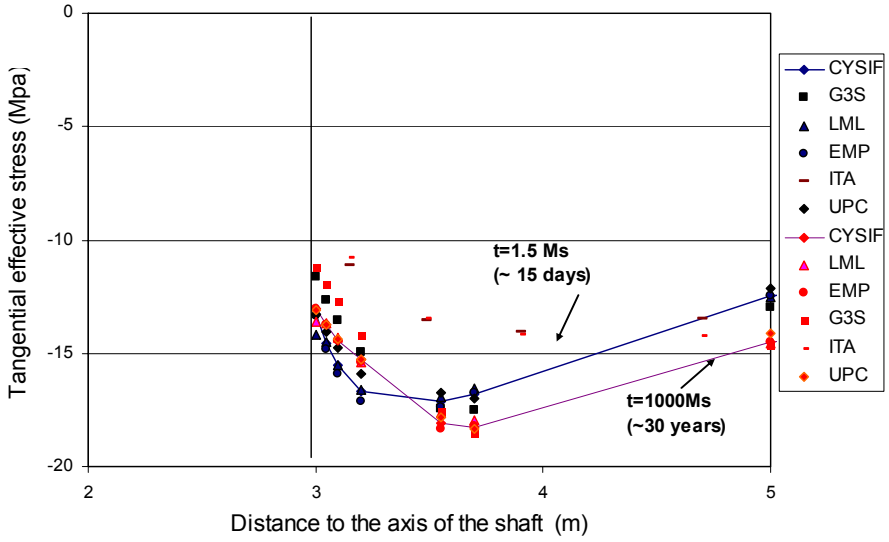

Figure 9. Comparison of tangential effective stresses immediately after excavation and 30 years later

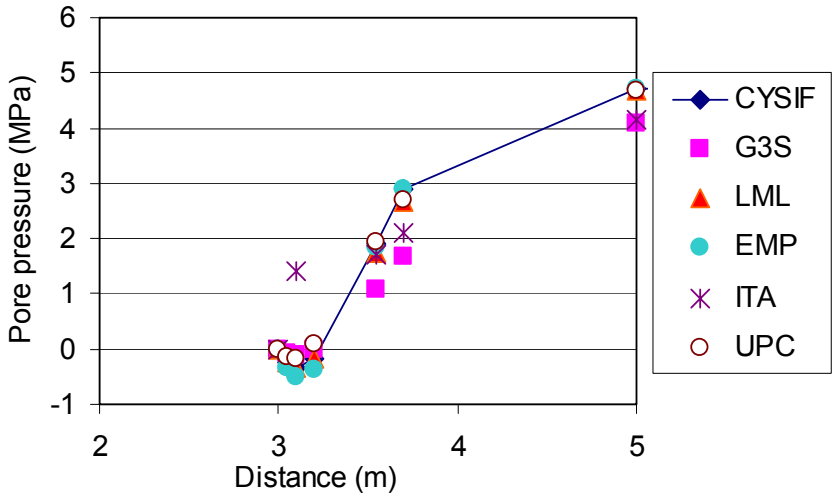

Figure 10. Comparison of pore-pressure distribution after excavation

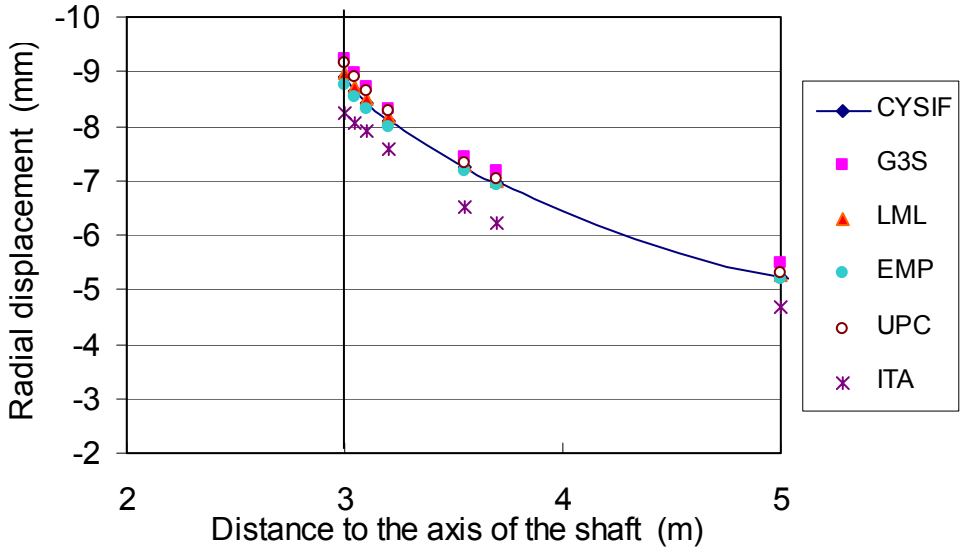

Figure 11. Comparison of radial displacements in the rock mass after excavation

4. CONSTITUTIVE MODELS DEVELOPED BY THE PROJECT

Based on observations and measurements of the argillite samples, three categories of rheological models were developed by research teams of the MODEX-REP project. Each category includes several mathematical formulations depending on the principal phenomena being considered by the model developers. Those models include:

- elastoplastic models (called EPE**)** in which the damage (non-linearity at a high deviatoric-stress level) and the post-rupture phase are simulated by a hardening of the initial plasticity criterion and a softening of the rupture criterion, respectively. Elastic properties remain constant during the transformation of the intact rock to the post-failure phase;
- damageable elastoplastic models (called EPD) based on the mechanics of the damages, where elastic properties change as a function of strain;
- a discrete model used by ITASCA (code PFC-AC/DC), simulating the mechanical behaviour by an assembly of particles.

4.1. Elastoplastic models with hardening and softening (EPE)

The EPE model was used by CGES, G3S, Andra, Nagra, SCK/CEN and Coyne-Bellier, is characterised by [3]:

- a plasticity criterion to simulate the start of the damage;
- a hardening of the damage criterion (initiation of plasticity) and a plastic flow potential to characterise the development of the plastic deformations before the rupture;
- a rupture criterion and a softening of the rupture criterion to reproduce the post-rupture behaviour of the material;
- an associated or non-associated plasticity flow law to calculate plastic deformations in order to characterise the damage and the cracking;
- a linear elastic behaviour under unloading conditions without elastic damage;
- hydro-mechanical coupling may be taken into account using the effective stress tensor in the criterion and the potential of plasticity flow (CGES, SCK/CEN and Nagra).

The proposed plasticity criterion is either derived from the Hoek-Brown criterion (Andra, SCK/CEN) or Mohr-Coulomb (Nagra, CGES, Coyne-Bellier).

Those models have the advantage of remaining simple with a limited number of parameters (no damage variable), while allowing the experimental curves of the saturated argillites to be easily reproduced. They are used to estimate the extension of the micro- and macro-fractured zone around an underground structure.

However, EPE models do not take into account the evolution of the elastic properties of the material, because the damage is addressed *via* the formulation of plasticity. They do not simulate the mechanical state of the material at the microscopic scale. Lastly, their plastic-flow potential is difficult to characterise from the tests on samples, because the elastic damage is not taken into account in the total deformation.

In the case of hydro-mechanical coupling, both effective stress and total stress approaches may be used. With such models, volume deformations generate variations in pore pressure (M→H coupling) and pore pressure has an impact on effective stresses (H→M coupling) on the start and development of the damage and the fissuring. The link is made between rock permeability and fissuring through the softening or hardening parameters calculated from the plastic-strain tensor.

4.2. Elastoplastic damageable models (EPD)

The EPD model, used by LML, LAEGO and CIMNE, is characterised by:

- an elastic damageable behaviour, characterised by a decreasing Young's modulus isotropically or anisotropically as a function of the intensity of the microcracks;
- a damage criterion, expressed in terms of elastic deformations;
- a plasticity criterion, dependent on the stress geometry;
- a coupling between the plasticity and the damage, by the simultaneous application of the consistency conditions between plasticity and damage criteria;
- an non-associated flow law to calculate irreversible plastic deformations;
- a poro-mechanical approach taking into account the pore pressure in the effective stress tensor.

The plastic load surface is parabolic and depends on the following three stress invariants: the damage variable, pore pressure and suction. The non-associated flow law describes the transition between the contraction and expansion observed on the volume-deformation curves of the tests. The post-rupture softening the argillites is reproduced by combining the damage model and the ideal plasticity criterion.

Those models take into account the degradation of the elastic properties of the argillites during loading. They separate the damage phenomenon (degradation of the elastic properties) from plasticity (irreversible deformations).

Similarly to EPE models, the plasticity and rupture-initiation criteria are based on an extension of the Drucker-Prager criterion. They depend on the three invariants of the stress tensor and the damage variable. The non-associated flow law describes the irreversible volume deformations.

The link between rock permeability and fissuring conditions is made through a damage parameter and the plastic deformation tensor.

The main problem in using those models is to determine the rupture and damage criteria of the argillites in terms of effective stresses. In fact, the tests on argillite samples consist to a large extent in undrained cases. Additional hypotheses are required to establish relevant criteria under effective stresses. The validity of those hypotheses remains nonetheless difficult to verify by tests on samples as well as by *in-situ* experimentations.

4.3. The discrete model – Simulation of rock behaviour by a particle assembly (AC/DC – PFC Code)

Contrary to the previous models, which are based on the mechanics of continuous media, the discrete model is based on a description of the medium represented as an assembly of spherical particles of varying diameters linked to one another by "cemented bonds", which reproduce

interparticle cohesion. Each contact of an interparticle is materialised by a so-called "parallel-bonded" material characterised by strength under traction and shearing. Thus, traction forces may be generated on these contacts, while physical contact is preserved between particles.

Roughly 10 elastoplastic parameters of the particles as well as the parallel bonds are required in order to define the macroscopic behaviour of the material. Those parameters include: (i) the normal and tangential rigidities of the particles; (ii) their friction coefficient; (iii) the normal and tangential rigidities of the parallel bonds and their strengths under traction and shearing. Those parameters were fitted by simulating triaxial compression tests on the argillites. The major problem in such an approach is to determine the microscopic properties of the contacts between particles in order to reproduce the macroscopic behaviour of the physical material. In that case, the representative behaviour of the material studied has to be determined before selecting appropriate microscopic properties *via* a fitting process.

The discrete model offers a good understanding of the phenomena, such as traction stress due to heterogeneity, the start of damage and the development of fissuring, as well as the localisation of fissures.

Table 4 provides an overview of the constitutive models proposed by the project's research teams. A large variety of approaches are used in different models. They may be considered as complementary in the sense that they reproduce different mechanisms acting in different situations.

Table 4. Overview of the constitutive models describing the short and long-term behaviour of the argillites for modelling the REP experiment

Research team	Short-term behaviour						Long-term behaviour	
	Model	**Damage/ plasticity**	**Damage criterion**	**Failure criterion**	**Post-failure**	**HM coupling**	**Creep model**	**HM coupling in creep model**
CGES	EPE	Plasticity – non-associated law		Mohr-Coulomb	Mohr-Coulomb	Yes	Lemaître	No
G3S	EPE	Hardening on extension	Von-Mises			Yes	New model	Yes
ITASCA France	Discrete – continuum	Bond strength	Bond strength	Bond strength	Bond strength	Yes	Differed Bond failure model	No
CIMNE/ ENRESA	EPD	Damage + plasticity	Ellipse in P-Q plan	Hoek-Brown		Yes	Viscoscalar damage model	Yes
Nagra	EPE	Plasticity – change of cohesion	Mohr-Coulomb	Mohr-Coulomb				
Andra	EPE	Plasticity – change of Rc	Hoek-Brown	Hoek-Brown	Hoek-Brown		Lemaître	No
LML	EPD	Damage + plasticity	P-Q	P-Q		Yes	New model	Yes
Coyne-Bellier	EPE	Plasticity	Mohr-Coulomb				Lemaître	No
SCK/CEN	EPE	Plasticity	Mohr-Coulomb				Lemaître	No

4.4. Simulation of uniaxial end triaxial compression tests

Figure 12 shows typical curves of compression tests obtained numerically with various constitutive models developed during the project. The strengths reproduced by various models are similar, but the strains at failure and their evolution after failure are quite different. That difference is mainly due to the various laws chosen for simulating the irreversible strain flow during pre- and post-failure phases. The approaches used by the different research teams to simulate damage, failure and associated irreversible strains are different: classical plasticity theory, damage mechanics theory, and discrete model.

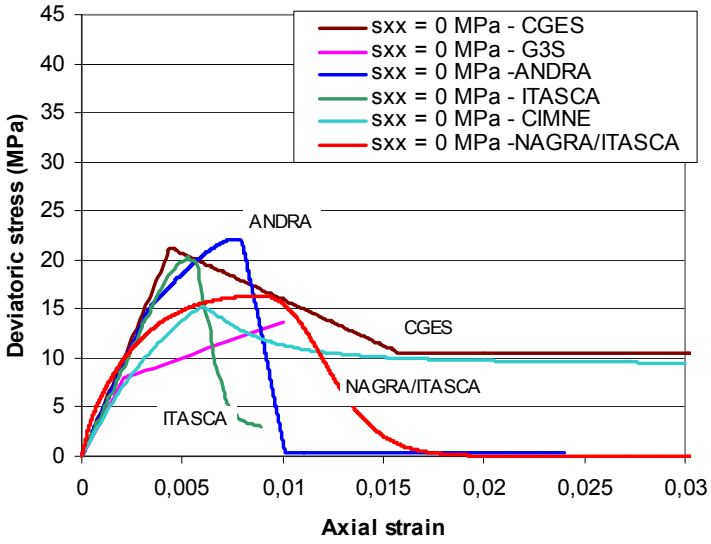

Figure 12a. without confining pressure

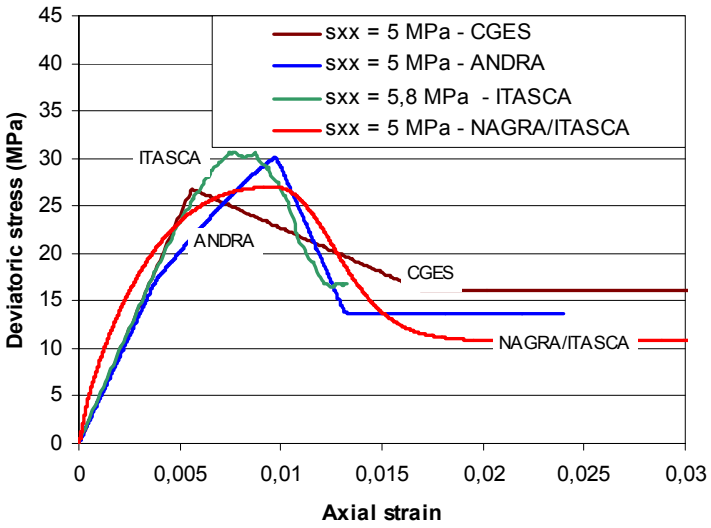

Figure 12b. with a 5-MPa confining pressure

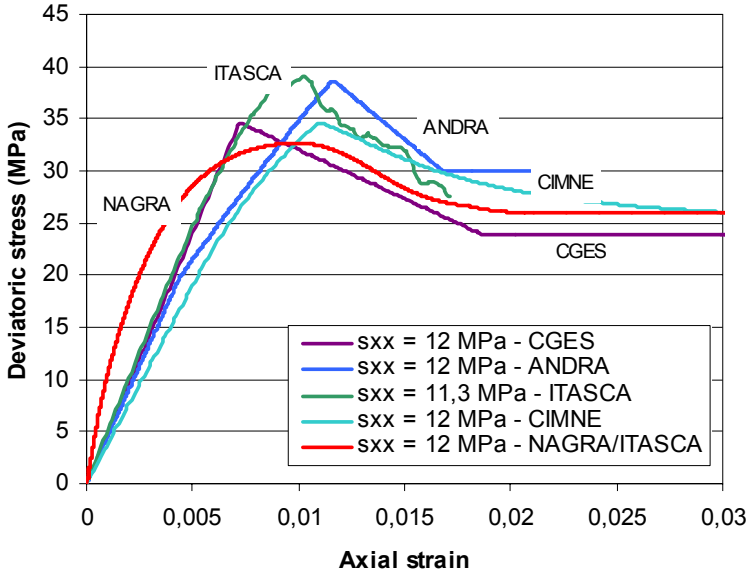

Figure 12c. with a 12-MPa confining pressure

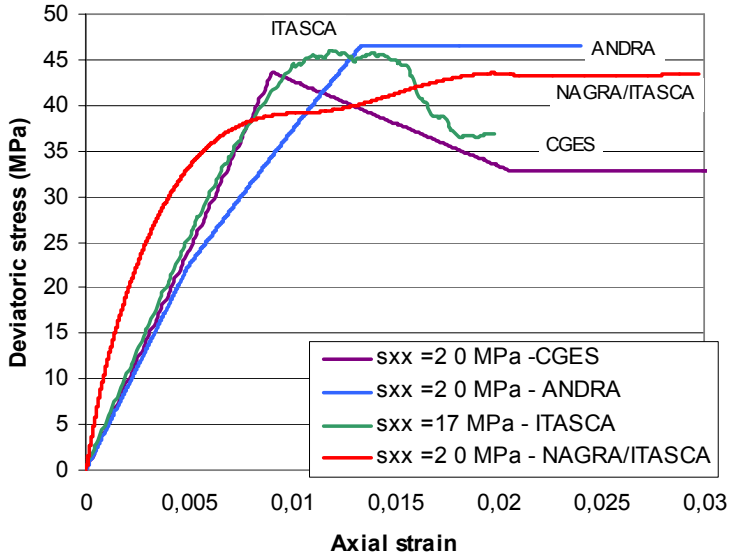

Figure 12d. with a 20-MPa confining pressure

Figure 12. Stress-strain curves of classical triaxial compression tests obtained by different constitutive models

4.5. Rheological models for time-dependent behaviour

Two types of time-dependent behaviour models were proposed in the MODEX-REP project for the argillites:

- viscoplastic models used by Andra, CGES, G3S, CIMNE, Coyne-Bellier, SCK/CEN, DBE, Nagra and LAEGO;
- deferred damage models proposed by LML and ITASCA-France.

➢ **Viscoplastic model**

Based on the creep-test results at ambient temperature, three formulations are proposed:

- Lemaître-type model (or a modified Norton-type model) initially proposed by Andra (Ghoreychi 1997, Gasc 1999);
- Burger-type creep model proposed by SCK/CEN;
- Salzer-type creep model proposed by Nagra.

The formulation and the associated parameters, as well as their reference values, proposed for the argillites are presented in deliverable 2 & 3 of the project [3]. Figures 11, 12 and 13 present the simulation of a creep test carried out on argillite sample EST5697-5. The comparison shows that the proposed viscoplastic models are able to simulate the strain evolution of the creep test for 4 months.

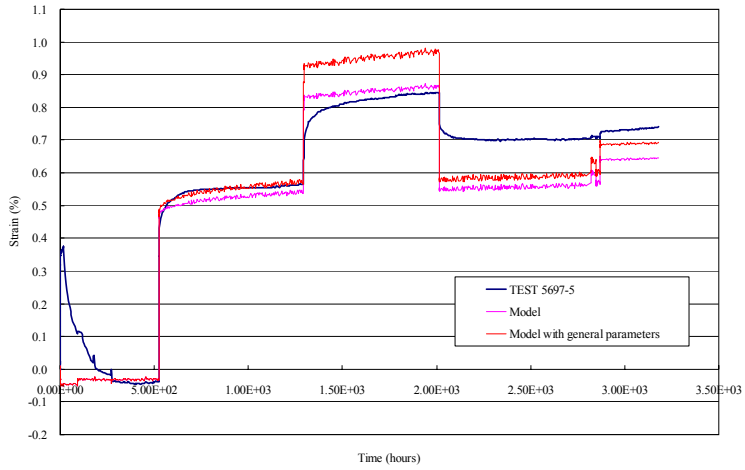

Figure 13. Comparison of simulation using Lemaître-type creep model and creep-experiment results on sample EST5697-5

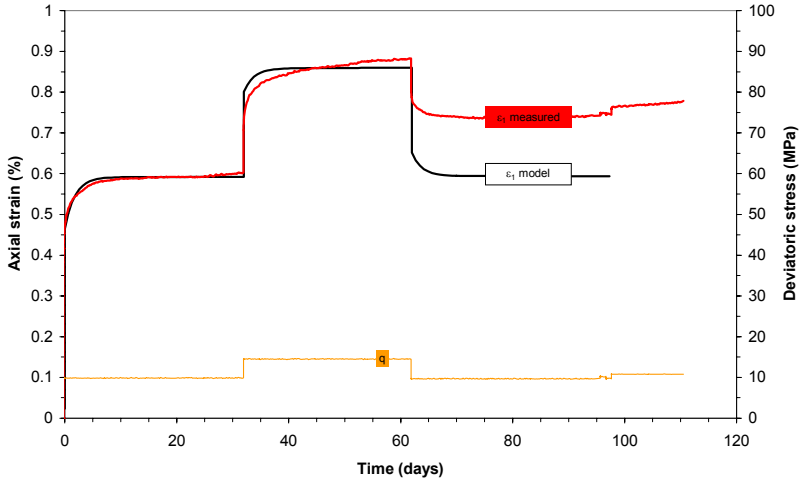

Figure 14. Comparison of simulation using Burger-type creep model and creep-experiment results on sample EST5697-5

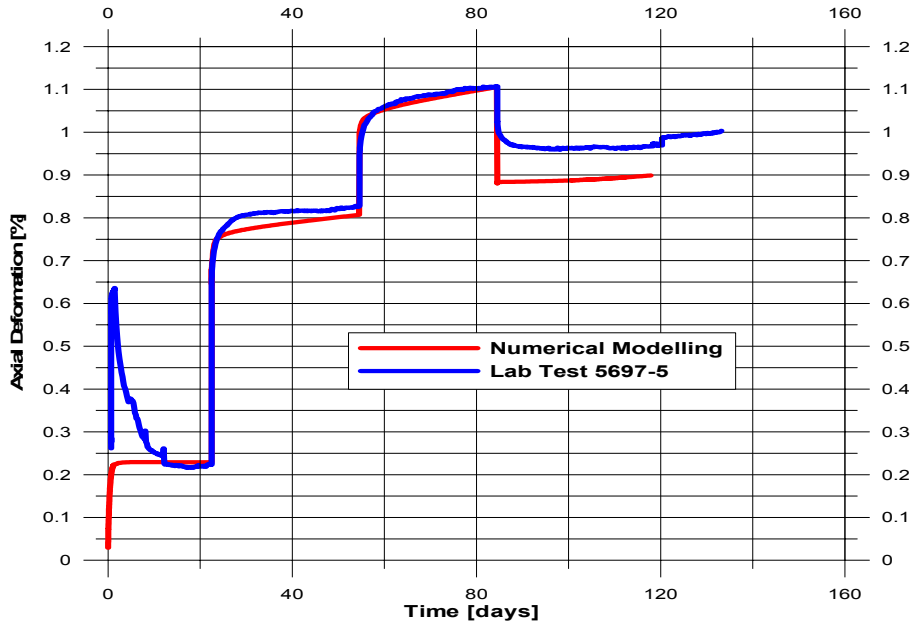

Figure 15. Comparison of simulation using Salzer-type creep model and creep-experiment results on sample EST5697-5

➢ Deferred-damage models

Within the project, two deferred-damage models for argillites were developed by LML and ITASCA-France, respectively.

Deferred-damage model proposed by LML

The LML deferred-damage model assumes that the deferred behaviour of argillites results from the evolution of microstructures over time: (i) the subcritical propagation of microfissures; (ii) the slow sliding of clay sheets; (iii) the progressive collapse of pores in the case of very porous rocks; and (iv) the chemical dissolution processes.

The base of the deferred-damage model is the short-term damage model (EPD model) developed by LML. For the quantitative representation of the evolution of microstructures over time, an internal scalar variable of the plastic deformations is introduced.

The parameters of the model for the argillites were fitted for several creep tests. The model has the advantage of not requiring a threshold to suppress the creep of the argillites outside the EDZ. The deferred deformation is not activated as long as damage has not started.

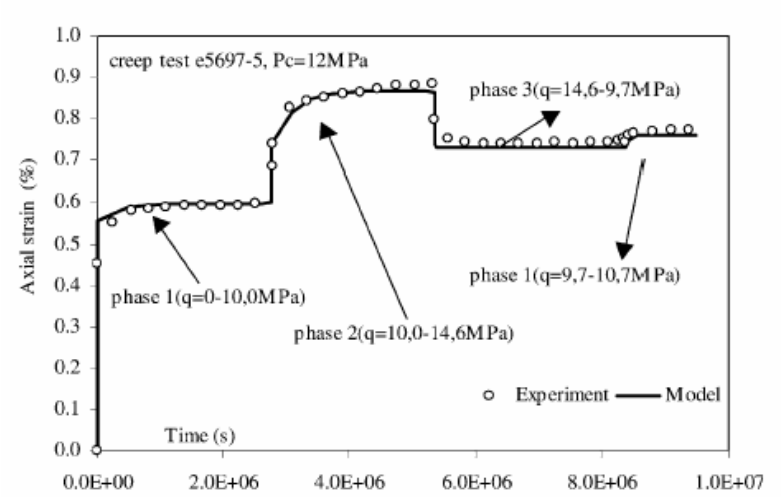

Figure 16. Comparison of simulations using deferred-damage models proposed by LML and creep-experiment results on sample EST5697-5

Deferred-damage model proposed by ITASCA

The representation of the long-term behaviour of argillites is based on the principle of the ageing of the connections (called "Parallel Bond") developed in each contact inter particle. When the shearing or tensile stress exceeds a threshold (parameter to be determined), the width of that connection is reduced by a coefficient, which is a function of the pressure applied to the connection. Reducing the width of that element causes the rigidity of the contact to decrease (and consequently, its module and its resistance) and, hence, to modify the forces being applied. That generates a new state of balance by reorganising the granular structure of the sample. Deformations are then induced. Parameters are determined by reproducing the creep tests carried out on argillite samples. Figure 17 represents a creep test, as well as the numerical simulation obtained by the deferred damage model. We note that the model can reproduce rather well the deferred deformation from the rock. However, it is difficult to define a single set of parameter able to reproduce the whole of creep tests, like that was noted by the whole of the teams working on the MODEX-REP project.

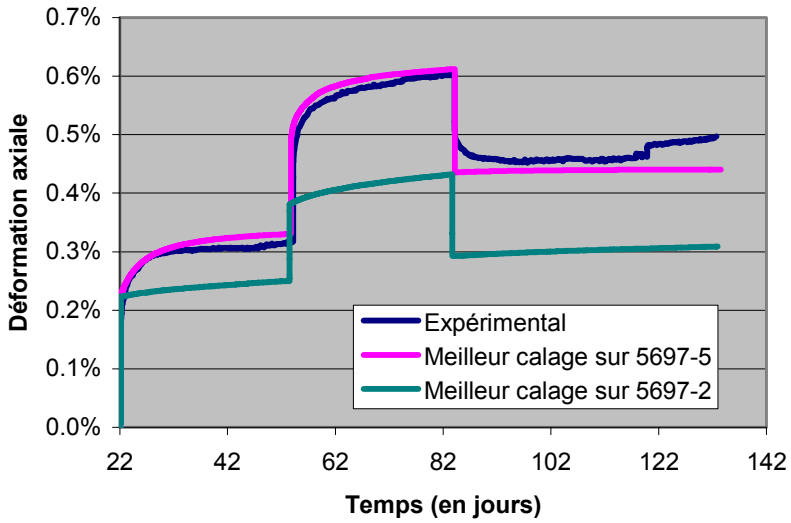

Figure 17. Comparison of simulations using deferred-damage models proposed by ITASCA and of creep-experiment results on sample EST5697-5

5. DESIGN AND SET-UP OF THE REP EXPERIMENT

5.1. Set-up of the REP experiment

The investigated zone for the REP experiment is located between 460 and 476 m in depth, where the secant modulus of the argillites is about 5 600 MPa and the uniaxial compression strength is 21 MPa in mean value. *In-situ* stress in the argillite layer is $\sigma_z = \gamma Z$, $\sigma_h \approx \sigma_v$, $\sigma_H / \sigma_h = 1,2 \sim 1,4$. The horizontal major stress is oriented NE, 155°.

For monitoring the hydro-mechanical response of the argillites to sinking operations, 15 instrumentation boreholes were drilled from the experimental drift (– 445 m) in December 2004 (Figure 18). About 120 hydro-mechanical sensors are placed in those boreholes as follows: 20 for pore pressure, 20 for displacements, four CSIRO 12-gauge cells for deformations, 10 for inclination and 27 piezoelectric sensors. Furthermore, two radial boreholes were specifically drilled at – 467 m for radial-displacement measurements behind the excavation face. Those sensors constitute a monitoring matrix for tracking the hydro-mechanical behaviour of the argillites.

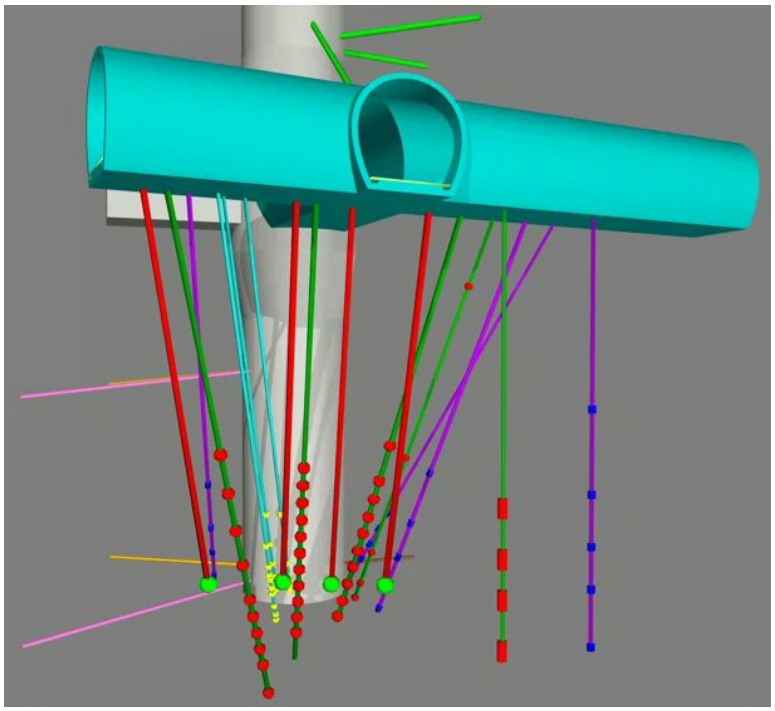

Figure 18. Layout of the REP experiment

The REP experiment consists of the following steps:

- Step 1: Drift excavation at the – 445 m level and instrumentation of the REP zone (July-December 2004). The drift is the starting point from which REP experiments are run. Sensors and measuring systems were installed in December 2004;
- Step 2: Stabilisation of sensors (December 2004 to February 2005): A sensor-stabilisation phase was required for all sensors, especially in the case of pore-pressure measurements;
- Step 3: Resumption of shaft sinking operations: Shaft advancement resumed on 10 March 2005, with the instrumentation matrix monitoring in real time the effects of the approaching working face.

5.2. Shaft-sinking method

The 6.1-m-diameter shaft was sunk according to a drill-and-blast method. The blast pattern was designed to excavate rock over a height of 2 to 3.1 m. Figure 19 shows a cross-section of the shaft in the REP study zone. The standard support system before application of concrete lining consists of 20 2.2-m-long bolts with wire mesh and shot crete in order to stabilise the rock wall and to prevent spalling.

Within the REP zone (between – 464.7 and – 469.7 m), the support system is replaced by six TH21/548 arches. Each arch is made up of five elements measuring 4.5 m in length (Figure 19). The arches are designed to slide with a friction force in the order of 120 kN.

The final lining consists of a layer of at least 0.5 m of B45 concrete injected by 6-m plots at a time. The distance between the final lining and the working face ranges from 18 to 24 m, or even 30 m in certain cases.

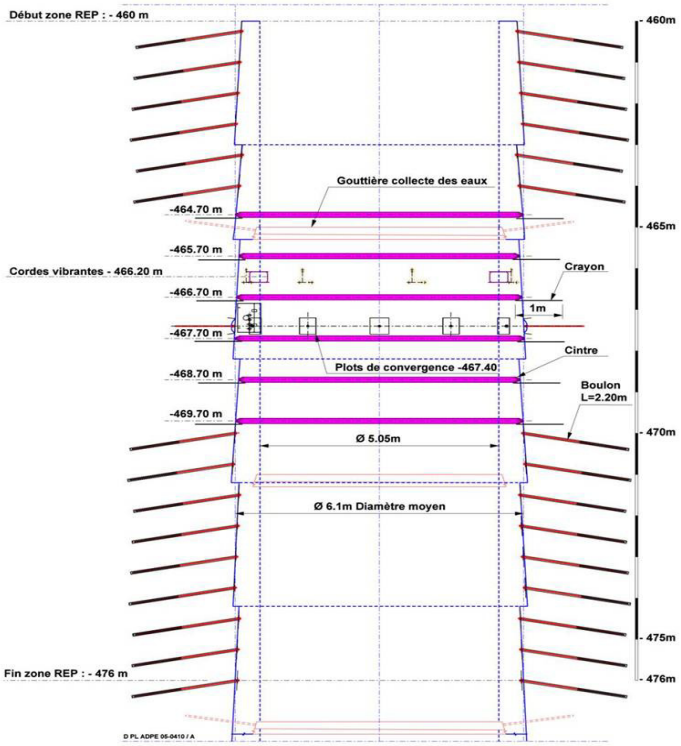

Figure 19. Cross-section of the access shaft between – 460 and – 475 m

5.3. Instrumentation

The optimal positions of the sensors are determined by taking several factors into consideration: (i) the over-excavation risk, (ii) the *in-situ* stress anisotropy and (ii) the variation range in the expected hydro-mechanical parameters. The accurate locations of the sensors are determined on the basis of the trajectory survey of the boreholes.

5.3.1. Pore-pressure measurements

Four boreholes are dedicated to pore-pressure measurements and to permeability tests. In three of them (REP2101, REP2102 and REP2103 – see Figure 20 and 22), the measuring points are located around the shaft at distances of 1.08 to 4.88 m from the theoretical wall. Boreholes are 101.3 mm in diameter and the theoretical volume of each interval between packers is 264.14 mL.

The fourth borehole (REP2104) is located outside the influence zone of the shaft (the distance from the shaft wall exceeds 13 m) and serves as the reference point for measuring initial pressure and permeability.

5.3.2. Displacement and strain

Two boreholes are fitted with multipoint extensometers (10 measuring points) in order to record rock displacements. The layout of boreholes REP2201 and REP2202 (Figure 20 and 22) is parallel to the main horizontal stresses. The measured displacement corresponds to the relative displacement of the anchoring with respect to the head of the boreholes.

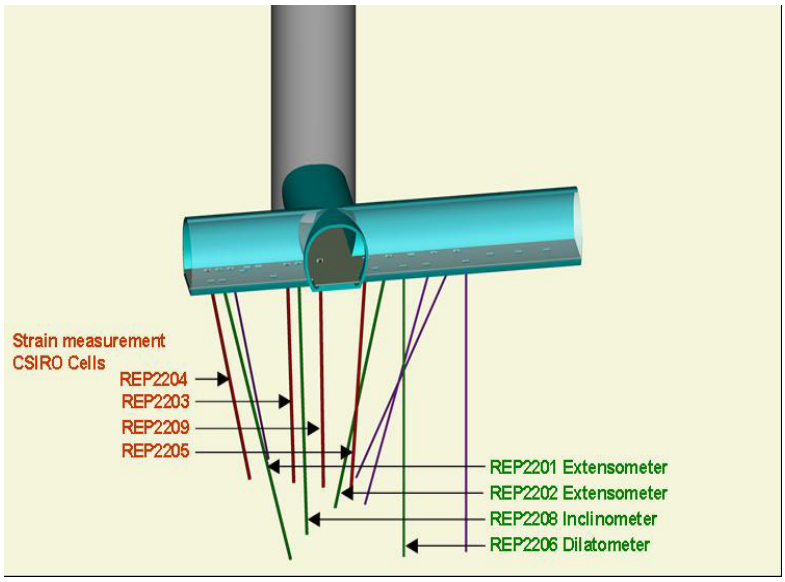

Figure 20. Geomechanical-monitoring boreholes

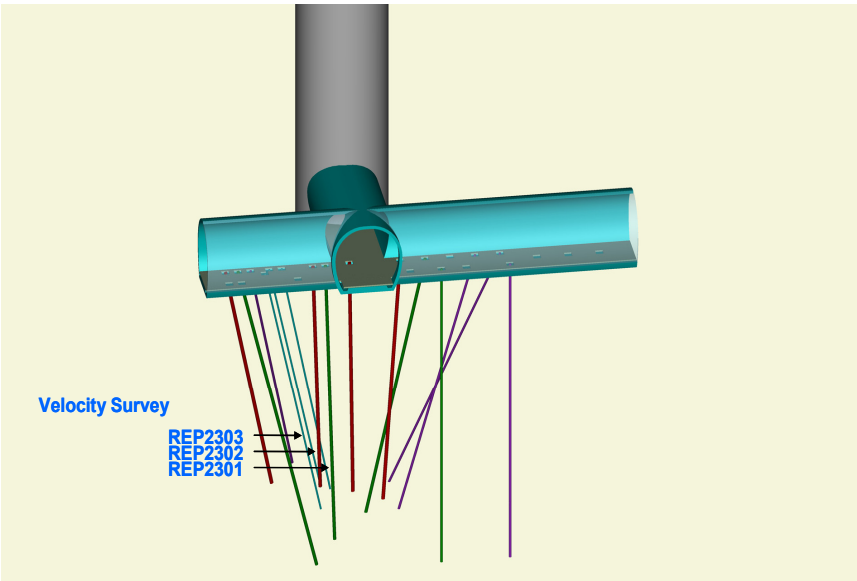

Figure 21. Velocity-survey boreholes

In addition, in both radial boreholes (PPA0031 and PPA0030) drilled from the shaft wall at – 467 m, displacement, permeability and ultrasonic velocity are measured. Shaft convergences are also measured after the passage of the drilling face at that level.

In three other boreholes (REP2203, REP2204 and REP2205) drilled from the drift at – 445 m level, soft-inclusion gauges have been installed to measure strain. Those CSIRO cell-type inclusions help to monitor the evolution of the strain field during shaft-sinking operations as well as deferred strain. The CSIRO Hi-12 cell is fitted in the rock within a pilot hole of 38 mm in diameter.

5.3.3. Velocity survey

The evolution of ultrasonic velocity is measured in boreholes REP2301, REP2302 and REP2303 during shaft-sinking operations (Figure 21). Those three boreholes are fitted with a system consisting of six to nine emitter/receiver sensors.

With the measurement system laid out in three boreholes, it is possible to transmit a total of 272 ultrasonic rays. However, due to the distribution of the system over 5 m and to the significant mitigation of the rock, the total number of recorded and interpretable rays (sufficient signal-to-noise ratio) amounts only to 115. Measurements were taken before and during shaft-sinking operations in order to characterise the evolution of velocities during sinking.

5.3.4. Overview of instrumentation matrix

Figure 22 shows the position of all sensors placed in the investigated volume of the REP experiment.

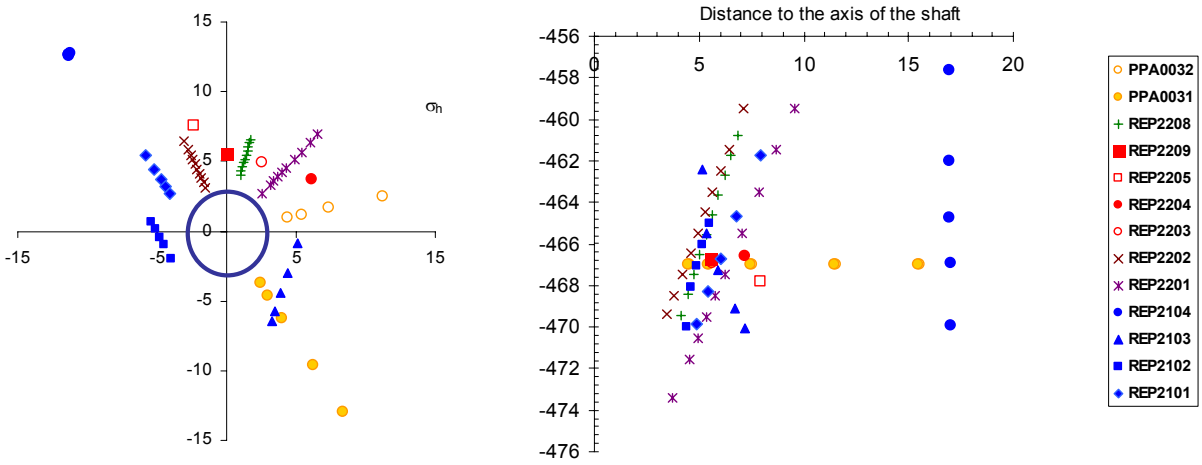

- *PPA0032 and PPA0031 radial boreholes drilled after the passage of the excavation face;*
- *REP2208 borehole for an inclinometer;*
- *REP2209, 2203, 2204 and 2205 boreholes hosted CSIRO sensor;*
- *REP2202 and 2201 boreholes for an extensometer;*
- *REP2101, 2102, 2103 and 2104 boreholes for pore-pressure measurements*

Figure 22. Position of sensors placed in the REP zone

6. BLIND PREDICTION OF THE REP EXPERIMENT

6.1. Blind prediction conducted in 2003

Early in 2003, the shaft had not reached yet the Callovo-Oxfordian argillite layer. According to the detailed construction schedule and the design of the REP experiment, the following parameters were set by Andra for the blind prediction of the argillite response to shaft-sinking operations [4]:

- shaft geometry;
- excavation method, support and lining mechanical characteristics;
- supposed excavation rate;
- theoretical position of sensors;
- general elastic properties of the argillites;
- initial pore pressure and *in-situ* total stresses.

In 2003, seven research teams participated in the blind prediction of the REP experiment. Table 1 shows the characteristics of the numerical models being used. Three of them (Andra, SCK/CEN and Nagra) called upon 3-D models, whereas the others proposed 2-D plane or 2-D axisymmetric models.

In the case of 3-D models, shaft-sinking is simulated step by step by deleting (muck) and adding (lining) mesh or changing mechanical characteristics of the relative volume excavated.

In the case of 2-D models, shaft-sinking is simulated by unloading progressively stresses and pore pressures on the shaft wall. In order to take into account the effects induced by the advance of shaft, ITASCA-France proposed to impose stresses and pore pressure calculated from an axisymmetric model on the 2-D plane model.

Table 2 summarises the main results obtained by numerical models. It shows that displacements predicted by the model on the shaft wall are:

- 12-20 mm (in radius) in total in the direction of the horizontal major stress (σ_H);
- 6-13 mm in the direction of the horizontal minor stress (σ_h).

If one considers that 30 % of those displacements occurred before the passage of shaft-sinking face, the measurable displacements on the shaft wall (in radius) behind the excavation face are:

- 8-14 mm in total towards the horizontal major stress (σ_H);
- 4-9 mm towards the horizontal minor stress (σ_h).

Tangential stresses on the shaft wall obtained by numerical modelling ranged between 12.5 and 22 MPa towards σ_h, and between 18 and 22 MPa towards σ_H. Since the rock mass adjacent to the shaft wall is almost in elastic state, the elastic properties of the rock mass control mainly the displacement and the stresses.

The extension of the micro-fractured zone, where irreversible strains appear, but the maximum strength of the rock has not been reached yet, is less than 1.0 radius of the shaft in the horizontal minor-stress direction and 0.3 radius in the major-stress direction,

The extension of the fractured zone, where the maximum strength of the rock is exceeded and macro-fractures may occur, is less than 0.1 radius of the shaft (forecasted by the Coyne-Bellier model).

Table 5. Overview of predictive modelling for the REP experiment conducted by MODEX-REP research teams

Research team	Main hypothesis	Numerical models
CGES	▪ Shaft advancement simulated by reducing the stress and pressure on the shaft wall ▪ Taking account HM coupling	▪ 2-D strain plane + 2-D axisymmetrical model
ITASCA	▪ Two models, one is for determining the initial state of the REP layer before excavation ▪ Shaft advancement simulated by reducing the stress and pressure on the shaft wall	▪ 2-D plane with given stress and 2-D axisymmetric, coupled modelling between FLAC and PFC codes ▪ three modelling steps of: (i) digging of the upper layers: obtain the new stress state (ii) excavation phase, (iii) lining phase and long-term behaviour
CIMNE/ ENRESA	▪ One excavation step	▪ 2-D plane strain ▪ Excavation in 1.5 days ▪ Temporal support: 7.5 days
Nagra	▪ Preliminary support modelled by an equivalent normal stress ▪ Final concrete represented by elements with time-dependent stiffness	▪ 3-D model (FLAC3-D) , ¼ of shaft ▪ Six lining segments ▪ HM coupling
Andra	▪ Excavation in 6 steps ▪ Liner takes contact with rock mass immediately after emplacement	▪ 3-D, ¼ of the shaft represented ▪ Elastoplastic model
Coyne-Bellier	▪ Isotropy of initial stress ▪ K_H=1.2 ▪ non HM coupling	▪ 2-D axisymmetrical model
SCK/CEN	▪ Only one part of the shaft (24 m high) considered ▪ With HM coupling	▪ 3-D model, ¼ of the shaft

Table 6. Overview of the numerical results of the REP experiment obtained by the MODEX-REP research teams

Research team	Mechanical results				Pore pressure	Extension EDZ	
	U_{47} (mm)	U_{66} (mm)	S_{47} (MPa)	S_{66} (MPa)	P_{19} (r = 4.7m) (MPa)	Fractured zone	Damaged zone
CGES	19	13.5	17	20	6	0	X: 1 m Y: 1.3 m
ITASCA	19	6	20	22	4.5	0	X: 0.3 m Y: 0.3 m
CIMNE/ ENRESA	19	13	12.5	19	7	0	1.8 m
Nagra	13	10			6	0	X: 1.0 m Y: 1.0 m
Andra	18	10	15	22			X: 0.6 m Y: 2.4 m
Coyne-Bellier	20	20	18	18		0.3 m	1.0 m
SCK/CEN	12	6			5	0	X: 0.3 m Y: 2.4 m

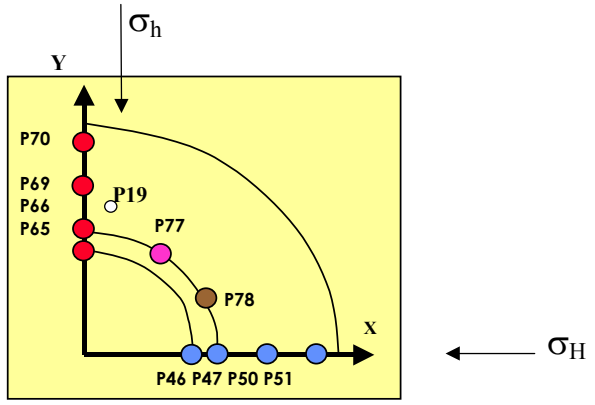

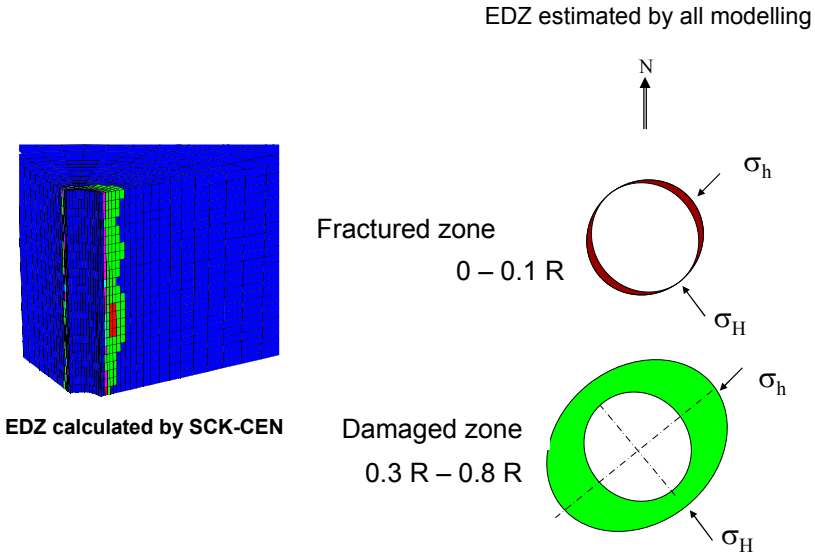

Figure 23. EDZ extension forecasted by MODEX-REP research teams in March 2003

6.2. Blind prediction conducted in 2005 and comparison with *in-situ* measurements

6.2.1. Numerical and constitutive models for predictive modelling

In June 2005, before the excavation of the REP section, a detail specification of predictive modelling of the REP experiment was prepared by Andra [5]. The following parameters were set by Andra for blind prediction:

- shaft geometry;
- excavation method, support and lining mechanical characteristics;
- actual excavation rate;
- actual position of sensors;
- elastic properties of the argillites measured in boreholes in the REP zone;
- initial pore pressure measured in the REP zone during the stabilisation phase and initial total stresses measured at the Bure site in 2004.

The blind prediction of the REP experiment was carried out by following teams:

- Coyne et Bellier;
- CIMNE/ ENRESA;
- Nagra (ITASCA Consultants GmbH);
- SCK/CEN;
- G3S;
- LML;
- CGES-ENSMP;
- ITASCA France;
- DBE;
- LAEGO.

The different numerical models include: three full 3-D models, one combined 2-D/3-D model, four 2-D axisymmetric models and two 2-D plane models. Seven numerical codes are used by

different teams and include: VIPLEF; ABAQUS, FLAC^{3-D}, PFC^{2-D}, Code_Aster, THMPASA, Code_Bright. Table 2 shows the main characteristics of the numerical models used for the blind prediction of the REP experiment.

Table 7. Main characteristics of numerical models for the REP experiment

	Nagra	**SCK/CEN**	**Coyne-Bellier**	**CGES/ ENSMP**	**G3S**	**LML**	**ITASCA**	**DBE**	**LAEGO**	**Cimne/ ENRESA**
Numerical code	FLAC^{3-D}	FLAC^{3-D}	FLAC^{2-D}	VIPLEF	Abaqus	THMPASA	PFC^{2-D}/ FLAC^{3-D}	FLAC^{3-D}	Code_Aster	Code-Bright
Key characteristic	Explicit FDM	Explicit FDM	FDM	FEM	FEM	FEM	PFC/FDM	Explicit FDM	FEM	FEM
Numerical model	Full 3-D	3-D	2-D axisymmetric	2-D plane strain	2-D axisymmetric	2-D axisymmetric	2-D plane/3-D model	3-D	2-D axisymmetric	2-D axisymmetric
Number of meshed and nodes	66,640 m 72,051 n	10,368 m 11,725 n	6,460 m 6,669 n	5,482 m 11,185 n	17,850 m 18,120 n	2,034 m 2,135 n	30000 particles	315,000 m 319,000 n	4052 m 10538 n	
HM coupling	HM coupled (Biot)	HM coupled (Biot)	No	M undrained conditions	HM with unsaturation	HM coupled (Biot)	HM coupled (Biot)	HM coupled (Biot)	HM coupled (Biot)	HM
Dependence of K with damage	×10 if □ p‡0	No	No		No	Yes, maxi ×1000	Yes	No	No	Yes
Method of simulation of excavation	Deleting elements	Inactivating elements	Inactivating elements	Unconfining ratio	Unconfining ratio	Unconfining ratio	Decreasing of stress sate	Inactivating elements	Inactivating elements	Unconfining ratio
E (MPa)	7,000	5,600	9,000	13,000	9,000	3,457	3,100	9,000	4,500	7,000
Rc (MPa)	16	28		21.2	20	21	41	25	7.3	15
Rheology for short term	EPE - MC	EPP-MC	Elastic	EPE	Elastic	EPD	Apparition of □ cracks	EPP Mohr-Coulomb	EPE	EPD
Creep	Salzer model (Q_0= 4.8 MPa)	Kelvin model	Lemaître model		–	Deferred damage		Norton	Lemaître	Deferred damage
Method of determination EDZ	Based on □ p	Based on □ p (□ & tension)	Post-treatment	Based on □ p	No	Based on □ p			Based on □ p	Moduli degradation
EDZ (thickness)										
Micro-fissuring (pre-failure)	4m (□ h) 3m (□ H)	0.7 m (□ h) 0.3 m (□ H)	0.6 m (□ h) 0.6 m (□ H)	Negligible	ND	2 m (□ h) 1.2 m (□ H)	None None	ND (□ h) ND (□ H)	1.15 m (□ h) 1.15 m (□ H)	5 m (□ h) 5 m(□ h)
Macro-cracking zone (post-failure)	0 (□ h) 0 (s_H)	0 (□ h) 0 (s_H)	0 (□ h) 0 (s_H)			0 (□ h) 0 (s_H)	None None	1.0 m (□ h) 0.7 m (s_H)	0.05 m (□ h) 0.05 m (s_H	

* EPE: Elastoplastic with softening and hardening model; EPP: Parfait elastoplastic model; EPD: Elastoplastic with damage model.

6.2.2. Comparison between blind prediction and in-situ measurements

- **Shaft convergence**

In general, numerical models tend to overestimate the shaft convergence measured behind the excavation face.

In-situ measurements recorded a shaft convergence of 11 and 9 mm in diameter towards σ_H, and σ_h, respectively, whereas the predicted convergence ranged from 10 to 20 mm and from 6 to 15 mm for both directions, respectively. The mean values supplied by the different numerical models are consistent with the measured convergence.

Among the different results, the following six teams supplied relatively good forecasts for the maximum convergence: G3S, CGES-ENSMP, LML, LAEGO, DBE and Nagra. In terms of the evolution of convergence over time, Nagra, DBE, LAEGO and CGES provided a relatively sound agreement with *in-situ* results. The numerical models without visco-plasticity underestimated the evolution of the displacement of the shaft wall over time.

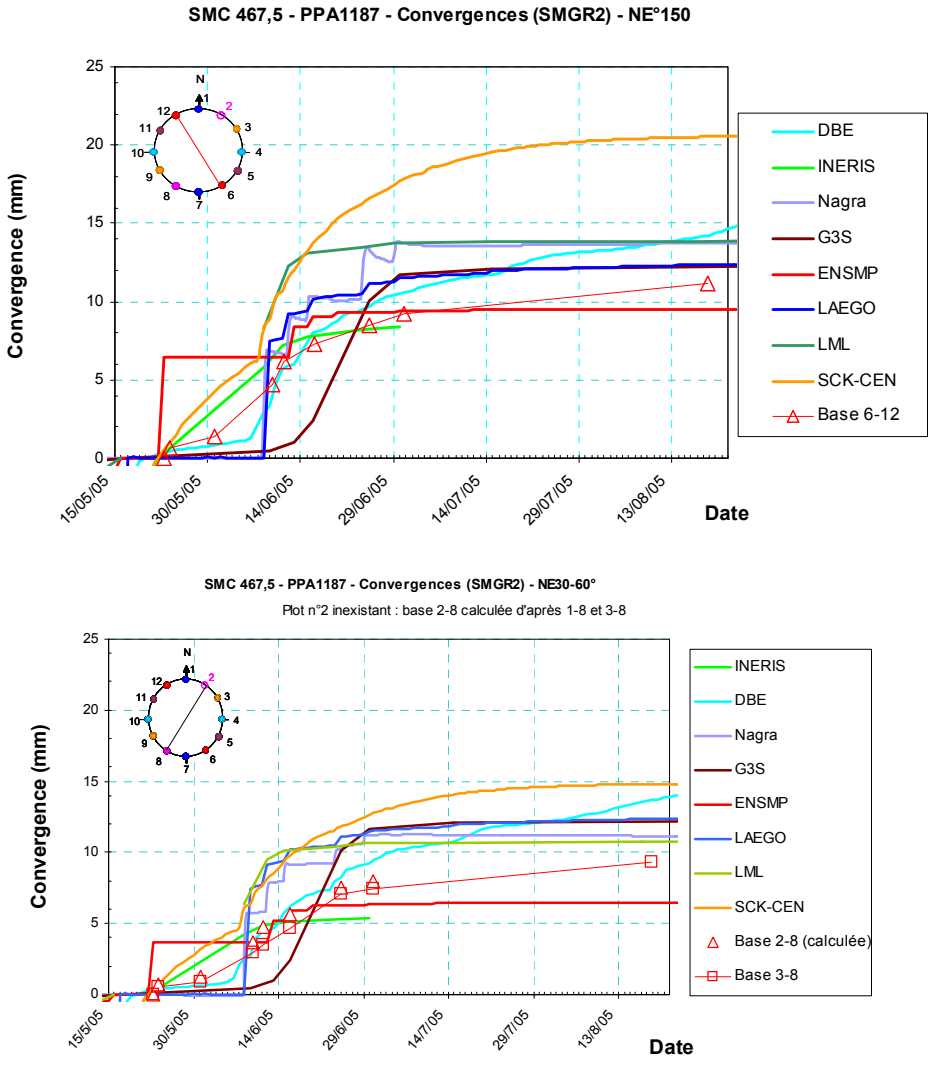

Figure 24. Comparison of shaft convergence between blind prediction and modelling

- **Displacement in the adjacent rock mass**

The numerical results supplied by the different teams are very scattered. Only LML, Nagra and SCK/CEN supplied relatively good agreement with measurements in some points.

Figure 25 shows the evolution of displacements within the rock as measured in borehole REP2202 compared with the head of the REP2202 extensometer.

Before shaft-sinking operations resumed, measurements were stable, which means that there were no relative displacements between anchoring points.

When shaft-sinking operations resumed, the shaft had reached a depth of 453.2 m and all anchorings of the REP2202 extensometer lay at least 6.20 m below that level.

As the working face progressed towards the REP zone, an initial compression phase was observed, followed by an extension phase. As long as shaft-sinking operations had not reached the anchoring level, the extensometer remained under compression. However, as soon as the shaft passed the anchoring level, the extensometer started to expand.

With regard to numerical modelling, only a few teams produced correctly the evolution tendency of two points (DFO10 and DFO9) (Figure 26 and 27). The results of the other teams were very scattered (Figure 27) and may be due to the post-treatment of numerical results for calculating the relative displacement.

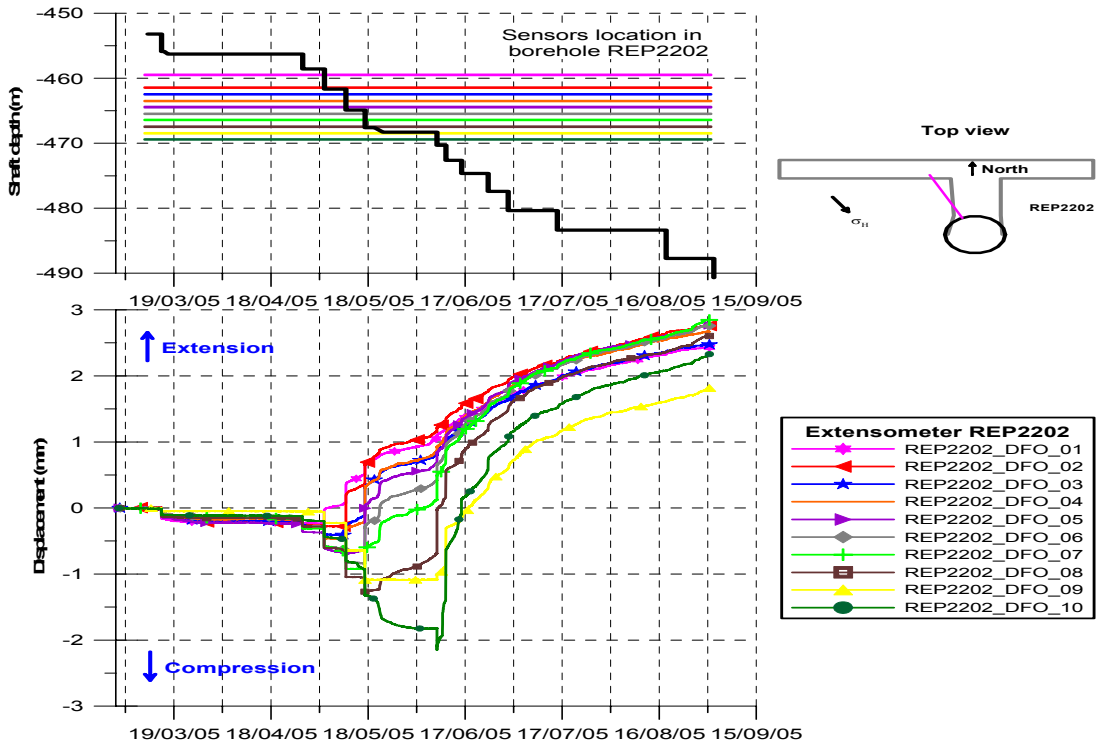

Figure 25. Measured displacements in borehole REP2202 [11]

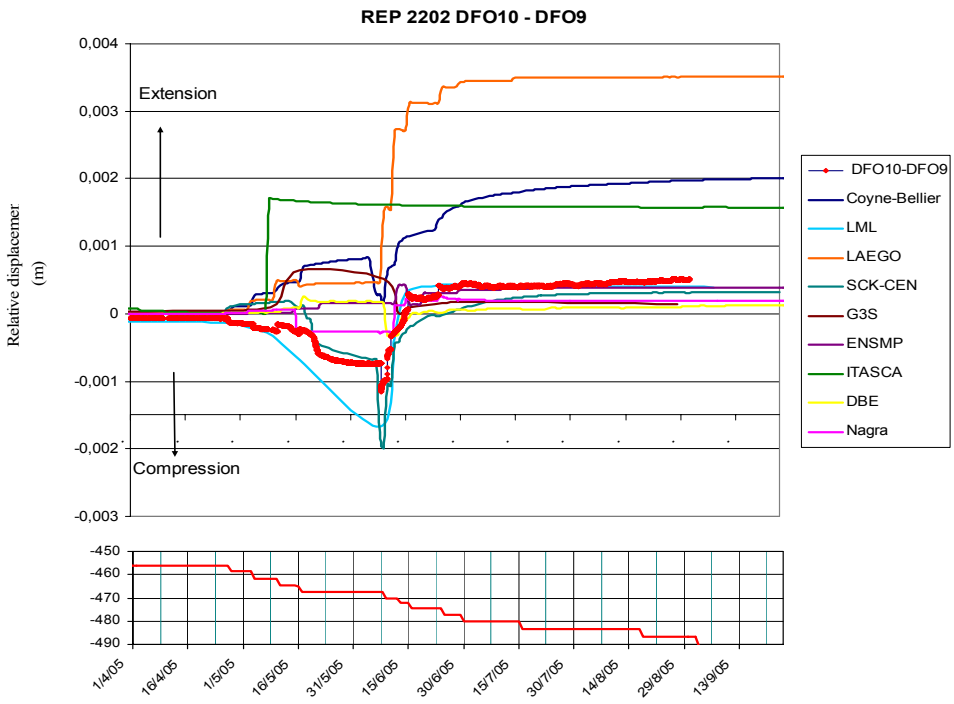

Figure 26. Comparison between measurements and predictions concerning the relative displacement of sensors DFO10 to DFO9 in borehole REP2202

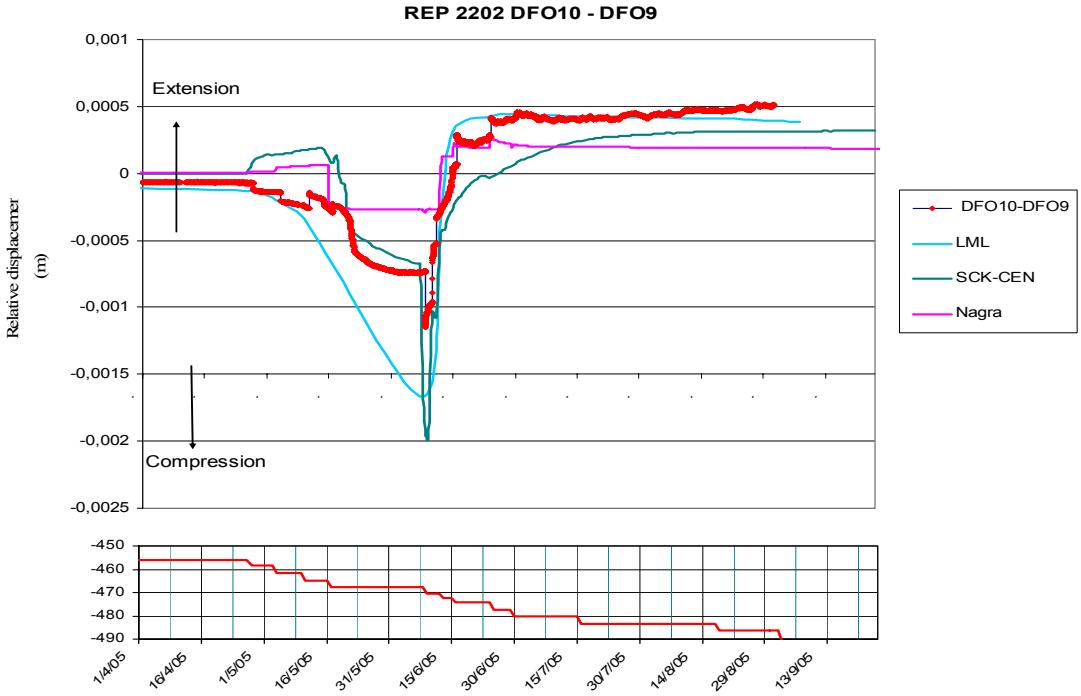

Figure 27. Comparison between measurements and predictions supplied by LML and SCK/CEN concerning the relative displacement of sensors DFO10 to DFO9 in borehole REP2202

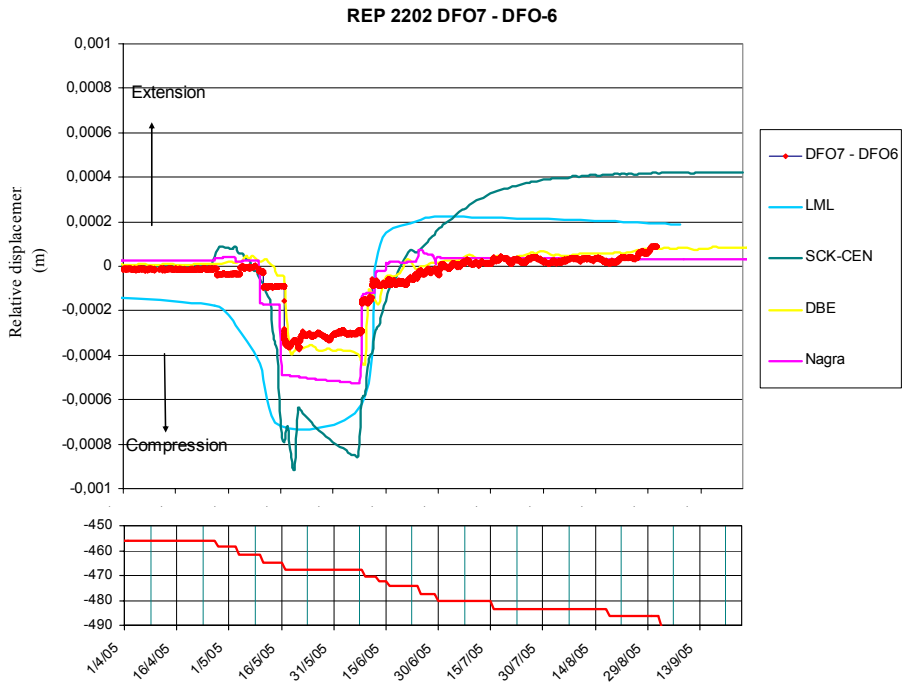

Figure 28. Comparison between measurements and predictions supplied by LML, DBE, Nagra and SCK/CEN concerning the relative displacement of sensors DFO10 to DFO9 in borehole REP2202

After the passage of the working face, measurement points do not return to their initial positions. A permanent extension is observed both with *in-situ* measurements and numerical predictions. However, only very slight variations were detected concerning the relative positions between sensors REP2202_DFO_1 to 8, which reflect a quasi-elastic behaviour of the rock mass in which those sensors are located. The behaviour of sensors REP2202_DFO_9 and 10 is different from the others. Their positions, close to the shaft wall (0.48 and 0.83 m, respectively), suggest that plastic deformations are induced within the argillite near the shaft wall.

The comparison demonstrated that the set-up of displacement measurement in the REP experiment was very precise. The small relative displacement (< 1 μm) between two bases of 1 m may be measured. That type of measurements supplied rich information about the mechanical status of the rock mass.

The displacements measured in borehole REP2201, oriented towards σ_h, are similar to those for borehole REP2202. A significant deferred displacement of that borehole head is observed, thus complicating considerably the interpretation and comparison of measurements collected in that borehole with numerical modelling.

- **Pore pressure**

The blind-prediction results for the evolution of the pore pressure are very scattered. SCK/CEN, UPC, LML, LAEGO, Nagra and G3S teams provided a relative good agreement with *in-situ* measurement in some observation points.

G3S studied desiccation phenomena due to ventilation. Pore pressure in the near-field decreased much more rapidly than the measurements. LML considered the change of permeability in the

EDZ (EPD-elastoplastic with damage model). Their results reproduced approximately the pressure evolution in some points. For other teams, the pore-pressure decreases were underestimated.

In-situ measurements show that before shaft-sinking operations resumed, pore pressures were almost constant at 3.4 to 3.9 MPa (
Figure 29). The first blast generated a small reduction in pressure, followed by a new stabilisation. The variation had an amplitude of 0.01 and 0.09 MPa for the furthest and nearest pressure-measurement chamber from the working face, respectively. Successive blasts induced an instantaneous variation in the pore pressure. The amplitude of those jumps increased in proportion to the proximity of the working face with the chamber level. In the forecasts, slight pore-pressure decreases before the passage of the excavation face were not reproduced, which mean that the pressure drop in those boreholes may be due to blasting.

The most significant reduction was observed when the shaft passed the level of the measurement chamber and the amplitude of drop increased when the wall was close to the chamber. It varied between 0.29 MPa in Chamber No. 1 at 4.85 m from the wall and 0.69 MPa in Chamber No. 5 at 1.7 m from the wall (Figure 29). That type of coupled hydro-mechanical behaviour was observed systematically in boreholes REP2101, 2102, and 2103 (Figure 31). In general, the numerical predictions underestimated the instantaneous pressure drop when the sinking face passed the level of the pressure sensor.

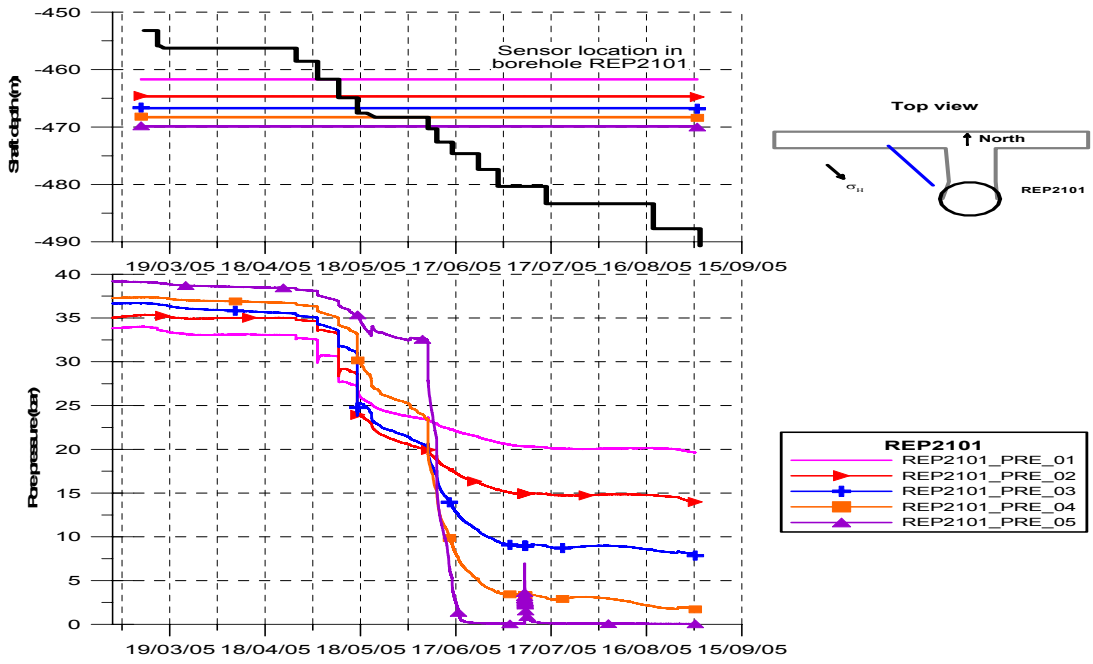

Figure 29. Evolution of pore pressures in borehole REP2101

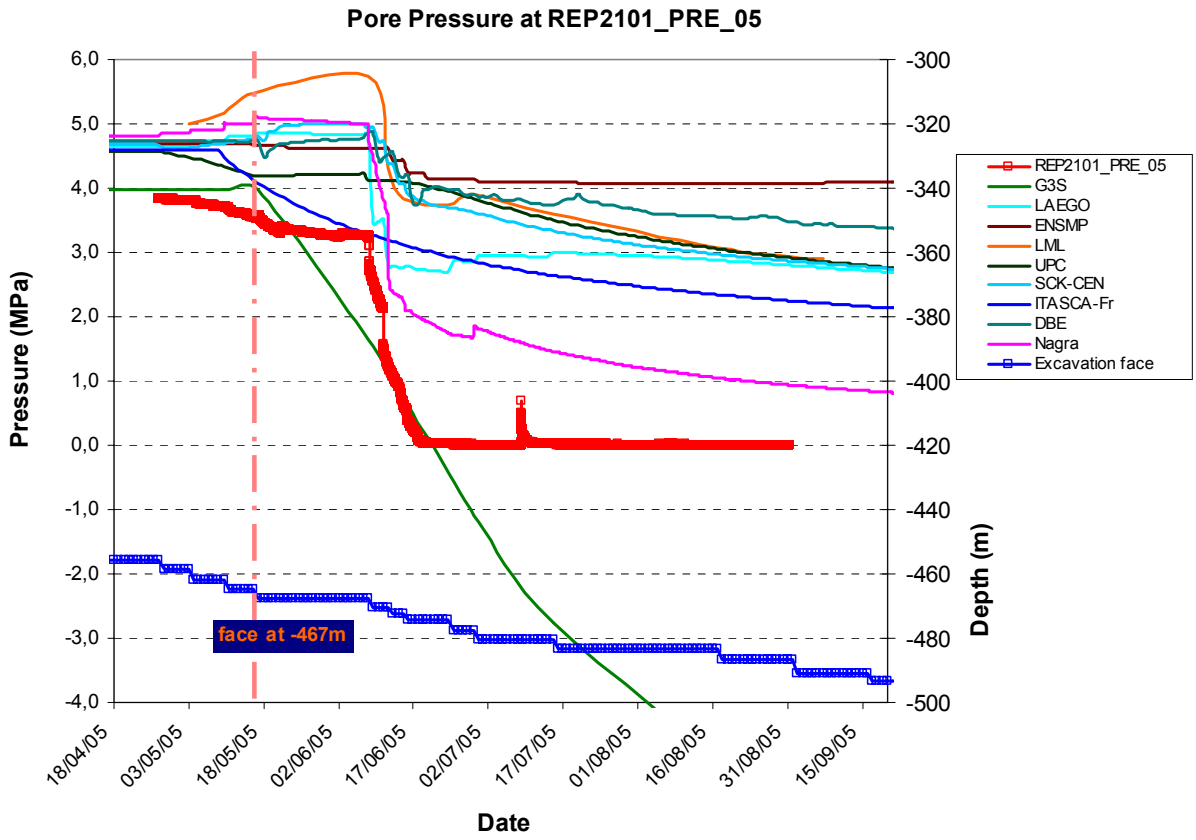

Figure 30. Comparison between pore-pressure measurements and predictions on point REP2101-PRE05

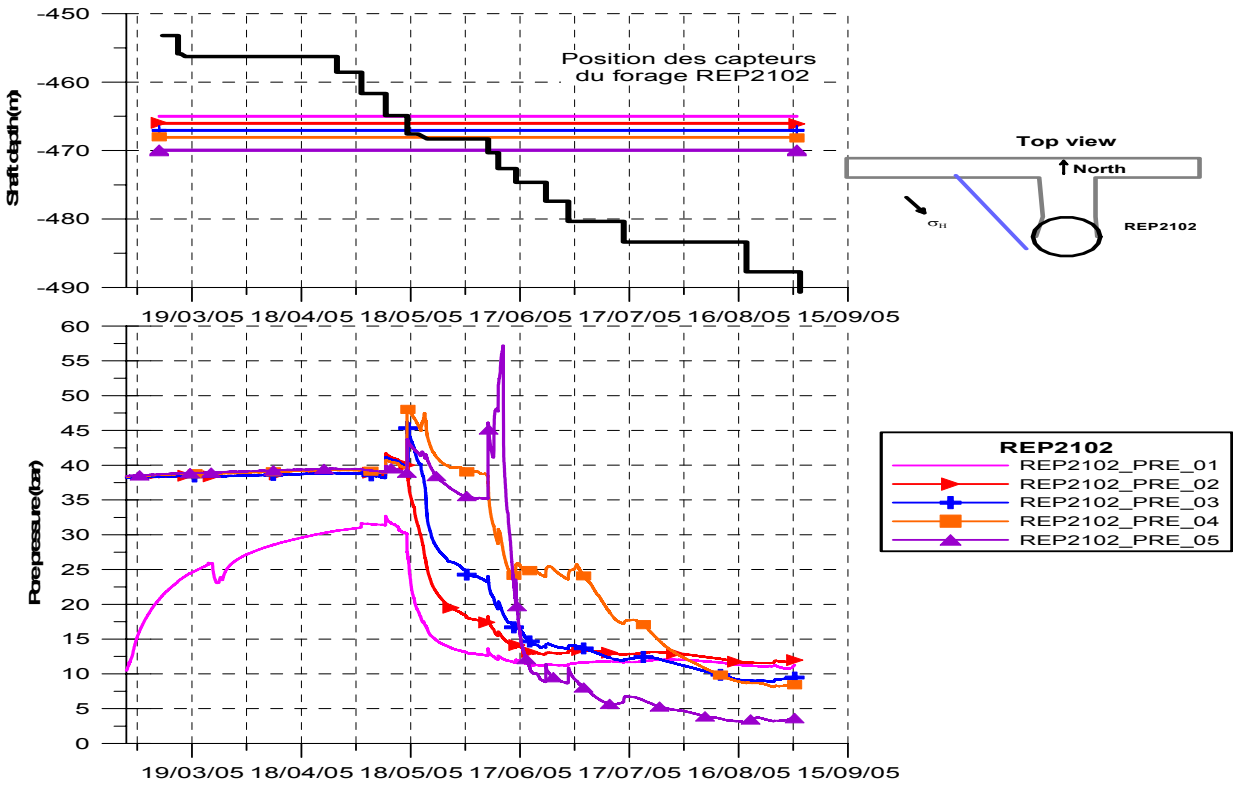

Figure 31. Evolution of pore pressures in borehole REP2102

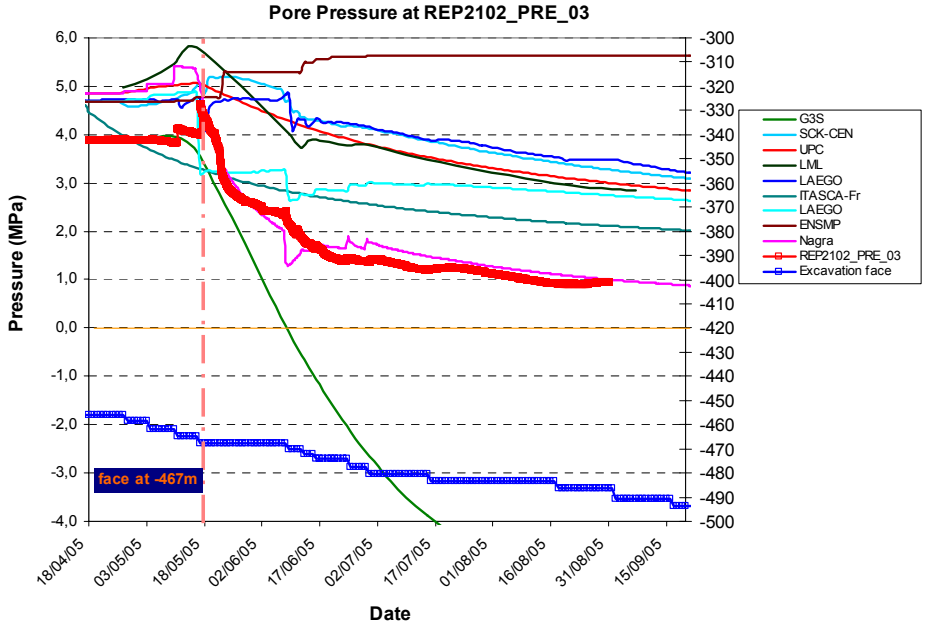

Figure 32 Comparison between pore-pressure measurements and predictions on point REP2102-PRE03

Figure 34 shows a comparison of the evolution of pore pressures in borehole REP2103 (chamber PRE01). The borehole is oriented rather towards of the minor horizontal stress.

The pressure variations measured in the chambers depend also on their position regarding the *in-situ* stress orientation. Overpressures were observed in some chambers in boreholes REP2102 and REP2103, when they were located in the area towards σ_h. Blind prediction (LML, CIMNE-UPC, Nagra, and LAEGO) produced also that type of evolution, but the production date of overpressures was poorly represented.

After the passage of the excavation face, the gap widened between measurements and forecasts concerning the pore-pressure amplitude. However, one may note that the evolution slope over time is quite similar. It may signify that water permeability ($K_{//}$ = 5.0 x 10^{-20} m^{-2} $K_{\perp}$ = 5.0 x 10^{-21} m^{-2}) used in the forecast is in consistent with the real case.

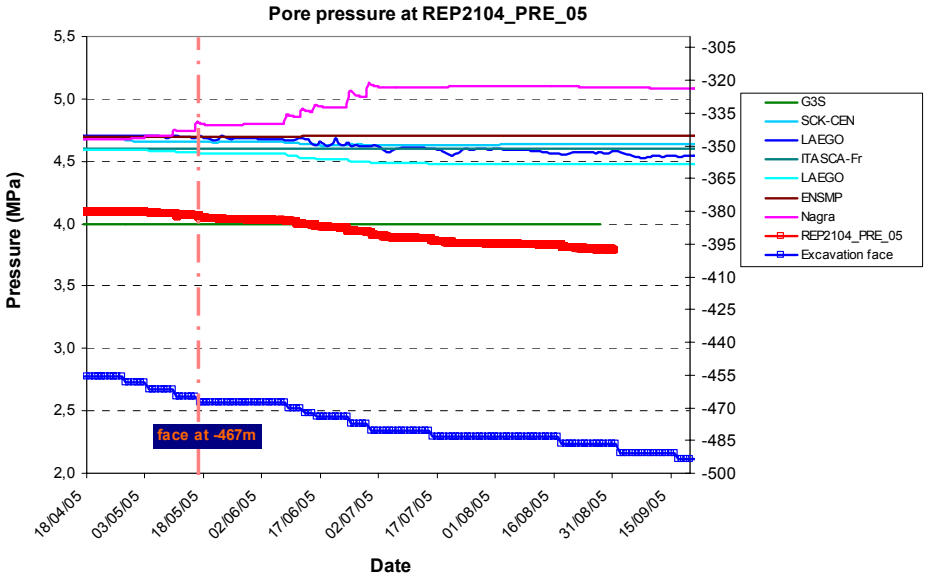

Figure 33. Comparison of the pore-pressure evolution measured in borehole REP2104

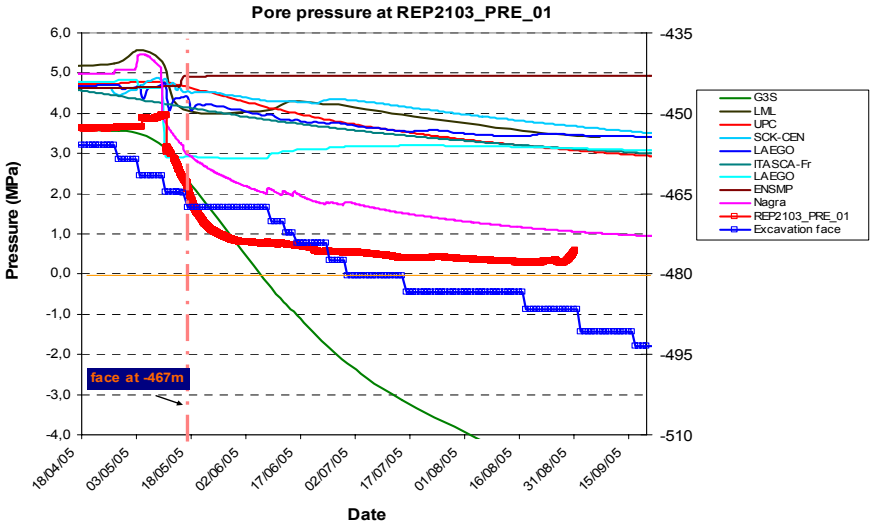

Figure 34. Comparison of the pore-pressure evolution measured in borehole REP2103-PRE-01

7. INTERPRETATIVE MODELLING OF THE REP EXPERIMENT

7.1. Improvement of numerical modelling proposed after blind prediction

Based on the analysis of the discrepancies observed between forecasts and measurements, improvements of numerical modelling of the REP experiment were carried out as follows:

7.1.1. Initial pore pressure

According to *in-situ* measurements, the initial pore pressure recorded in the REP zone was about 4 MPa.

7.1.2. Water permeability in the near-field

In-situ permeability measurements carried out in boreholes REP2101, REP2102, REP2103 and REP2104 show that the permeability of the intact argillites (before excavation) ranges from 4.0×10^{-21} m^{-2} to 7.0×10^{-20} m^{-2}. Those values are consistent with the values given in the modelling specification [5]: $K_{//} = 5.0 \times 10^{-20}$ m^{-2} and $K_{\perp} = 5.0 \times 10^{-21}$ m^{-2}.

Figure 35 shows the evolution of water permeability as measured after excavation in the adjacent argillites near the shaft wall. One may observe that the permeability increases in that zone in comparison to intact rock. A suitable power function to fit the *in-situ* data is proposed. That function leads to link the damage with the permeability evolution as follows:

$$\frac{K}{K_0} = 13.6 \times 10^{-0.2323\,d} \quad \text{for } d < 4.85 \text{ m}$$

where:

d is the distance to the shaft wall, d < 4.85 m
K_0 is the initial permeability.

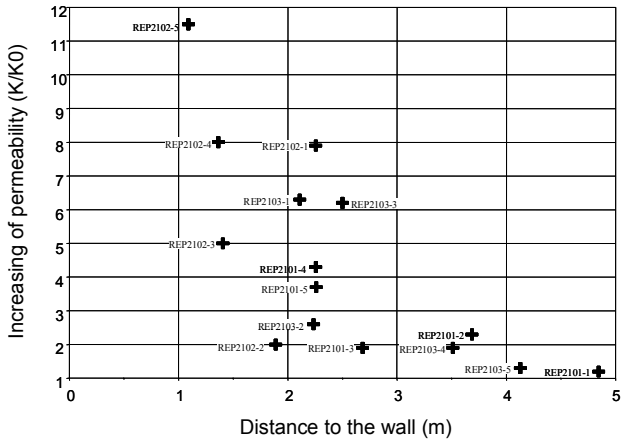

Figure 35. Permeability evolution after excavation (K) compared to the initial values measured before excavation (K_0) in the near-field of the shaft [11]

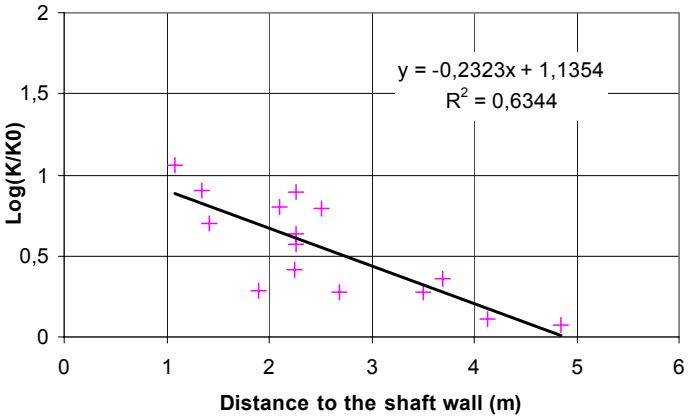

Figure 36. Evolution of permeability after excavation (K) compared to the initial values measured before excavation (K_0) in the near-field of the shaft

7.1.3. Elements for improving constitutive models

With regard to the blind-prediction results, the following facts were observed during the REP experiment and have been emphasised in order to improve the constitutive models of the investigated rock:

- argillite deformations in the REP zone are small. Towards the horizontal major stress (N155°), the rock mass presents a quasi-elastic behaviour since the displacement and shaft convergence in that direction may be reproduced by an elastic model;
- the displacements measured towards the horizontal minor stress show the creation of a plastic zone, but its extension is less than 1 to 2 m;
- the change of sound velocity in the near-field of shaft of the REP zone is less than 2 %, and is not significant;
- a significant pore-pressure drop was measured in the near-field of the shaft (~ 4 m), when the excavation face passed the level of pressure chamber;
- pore-pressure variations depend on the measurement position with respect to the horizontal stress orientation.

7.1.4. Precision of *in-situ* measurements

In order to improve the constitutive model and to diminish gaps between measurements and numerical models, the precision or reliability of *in-situ* measurements is graded (from high to low) according to the nature of the measurement, the operations carried out before, during and after the REP experiment for various sensors as well as the incidents that occurred during the experiment:

1. displacement measured in boreholes REP2201, REP2202, REP2203, REP2204, REP2205, REP2206, REP2207, REP2209 and REP2208;

2. pore pressure in boreholes REP2101, REP2102, REP2103 and REP2104;

3. shaft convergence;

4. displacement in vertical borehole PPA0027;

5. radial displacement in boreholes PPA0031 and PPA0032.

7.2. Interpretative modelling and comparison

Based on the above-mentioned elements, improvements in numerical modelling and constitutive models of argillites have been brought by MODEX-REP research teams after blind prediction. They are summarised in Table 8.

The following nine modelling teams participated in interpretative-modelling activities between October 2005 and February 2006:

- Andra-INERIS;
- Coyne-Bellier;
- Nagra;
- SCK/CEN;
- LML;
- CGES;
- ITASCA;
- LAEGO;
- DBE.

CIMNE-UPC had performed modelling after that period.

The new comparison between models and measurements was made on 22 February 2006 (seventh progress meeting).

Table 8 presents the main characteristics of numerical models and constitutive models used for interpretative modelling.

7.2.1. Comparison of shaft convergence

Compared to the blind prediction conducted in 2005, the shaft-convergence amplitude provided by numerical models is significantly reduced. Several teams reproduced correctly the shaft-displacement evolution: Coyne-Bellier, Andra-INERIS and DBE.

Coyne-Bellier recalibrated the parameter of Lemaitre's creep law by using the measured shaft convergence and was able to produce the best convergence reproduction.

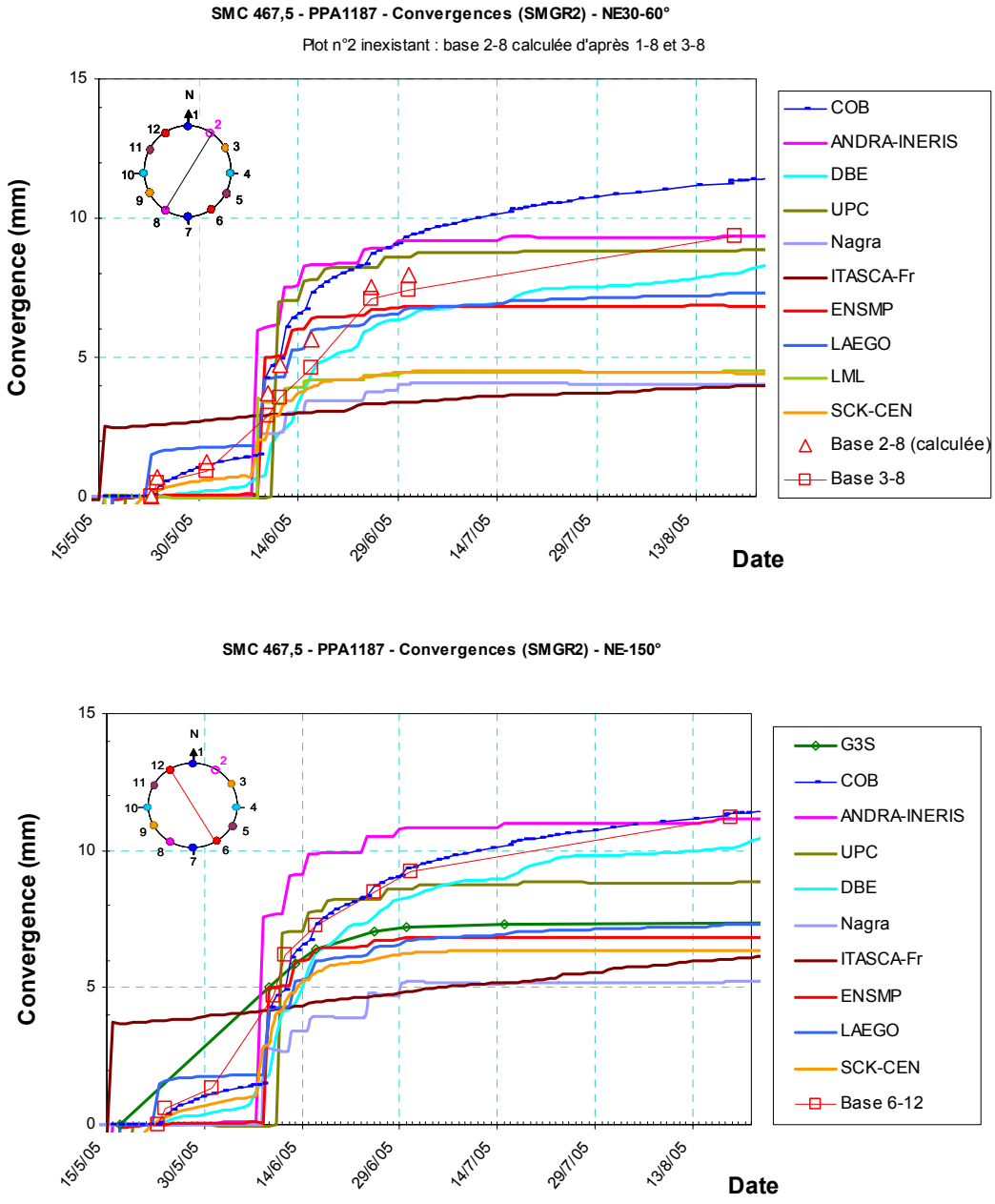

Figure 37. Comparison between measurements and interpretative models of shaft convergence in the REP section

7.2.2. Displacement of adjacent rock mass

All numerical models used for interpretative modelling reproduced correctly the displacement-evolution pattern. The time-dependent model proposed by Coyne-Bellier, DBE, LAEGO and LML provides a good representation of the displacement evolution within the rock mass (Figures 38 and 39). Improvements in the results obtained by interpretative modelling were very significant.

The ITASCA results show irreversible deformations after the passage of the face, but *in-situ* measurements show that irreversible strain is very negligible.

Table 8. Main characteristics of prediction and interpretative modelling realised in 2005-2006

	Nagra	**SCK/CEN**	**Coyne-Bellier**	**CGES/ ENSMP**	**G3S**	**LML**	**ITASCA**	**DBE**	**LaEGO**	**Cimne/ ENRESA**	**Andra-Ineris**
Numerical Code	FLAC3D	FLAC3D	FLAC2D	VIPLEF	Abaqus	THMPASA	PFC2D/FLAC3D	FLAC3D	Code_Aster	Code-Bright	Flac3D
Principe	Explicit FDM	Explicit FDM	FDM	FEM	FEM	FEM	PFC/FDM	Explicit FDM	FEM	FEM	Explicit FDM
Numerical model	Full 3D	3D	2D axi-symmetric	2D plane strain	2D axi-symmetric	2D axi-symmetric	2D plane/3D model	3D	2D axi-symmetric	2D axisymmetric	2D plane variable
Nb of mesh and nodes	66 640 m 72 051 n	10 368 m 11 725 n	6 460 m 6 669 n	5 482 m 11 185 n	17 850 m 18 120 n	2 034 m 2 135 n	30 000 particles	315 000 m 319 000 n	6 059m 18 490 n		318 390m 336 120n
HM coupling	HM coupled (Biot)	HM coupled (Biot)	non	M undrained conditions	HM with unsaturation	HM coupled (Biot)	HM coupled (Biot)	HM coupled (Biot)	HM coupled (Biot)	HM	HM coupled (Biot)
Dependence of K with damage	×10 if ‡0	non	non		non	Yes, maxi ×1000	Yes	non	non	HM	yes
Method of simulation of excavation	Deleting elements	Inactivating elements	Inactivating elements	Unconfining ratio	Unconfining ratio	Unconfining ratio	Decreasing of stress sate	Inactivating elements	Inactivating elements	Unconfining ratio	Inactivating elements
E (MPa)	7 000	5 600	9 000	13 000	9 000	3 457	9 000	9 000	4 500	7 000	5 600
Rc (MPa)	16	28		21	20	21	41	25	7.3	15	22
Rheology for short term	EPE - MC	EPP-MC	Elastic	EPE	Elastic	EPD	Apparition of cracks	EPP Mohr-Coulomb	EPE	EPD	EPE
Creep	-	Kelvin	Lemaître		-	-		Norton	Lemaître	Deferred damage	-
Method of determination EDZ	Based on	Based on (& tension)	Post-treatment	Based on	None	Based on			Based on	Moduli degradation	Based on
EDZ (thickness)											
Micro-fissuring (pre-failure)	4m (Δ_h) 3m (Δ_H)	0.7 m (Δ_h) 0.3 m (Δ_H)	0.6 m (Δ_h) 0.6 m (Δ_H)	Negligible	ND	1.24 m (Δ_h) 1.24 m(Δ_H)	None None	1.0 m (Δ_h) 0.4 m (Δ_H)	1.0 m (Δ_h) 1.0 m (Δ_H)	5.0 m (Δ_h) 5.0 m (Δ_H)	1.5 m (Δ_h) 1.5 m (Δ_H)
Macro-cracking zone (post-failure)	0 (Δ_h) 0 (s_H)	0 (Δ_h) 0 (s_H)	0 (Δ_h) 0 (s_H)				None None	0.4 m (Δ_h) 0.0 m (Δ_H)	0.1 m (Δ_h) 0.1 m (s_H	0.0 m (Δ_h) 0.0 m (Δ_H)	0.13 m (Δ_h) 0.13 m (Δ_H)
Improvement made in interpretative modelling	Non creep	Reduce creep b = 1 change of ini. and boundary conditions				Non creep + suction +change of Biot M	Re-calibration creep law Increasing K	Reduce creep	Modif. param. of model		

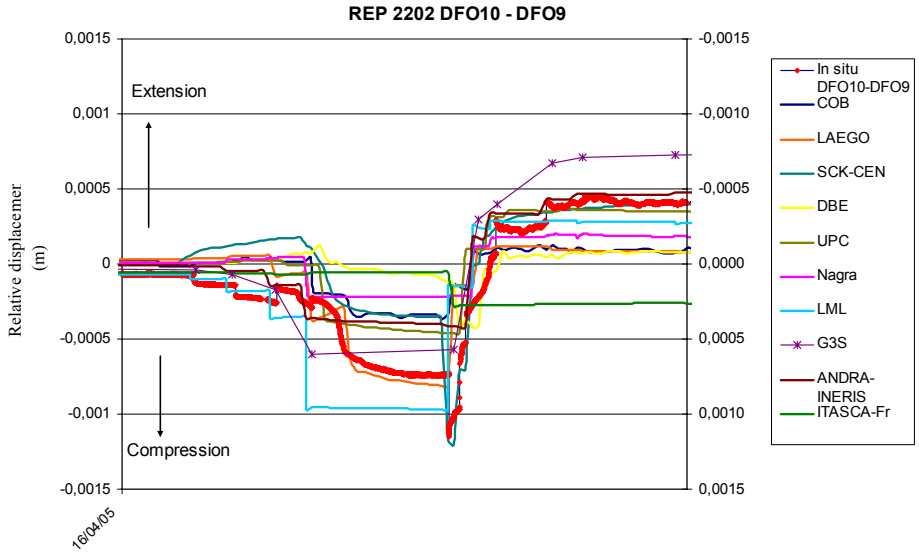

Figure 38. Comparison between measurements and interpretative models of relative displacements measured in borehole REP2202 (observations points: DFO10 and DFO9)

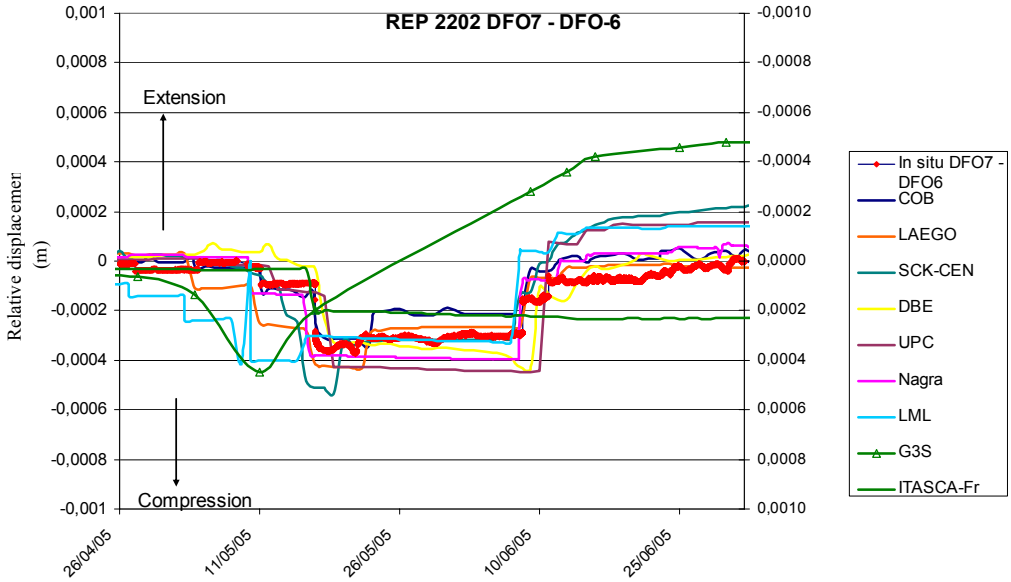

Figure 39. Comparison between measurements and interpretative models of relative displacements measured in borehole REP2202 (observation points: DFO7 and DFO6)

7.2.3. Pore-pressure evolution

A comparison of the pore-pressure evolution between interpretative modelling and *in-situ* measurement is shown in Figure 40, Figure 41, and Figure 42. One may observe the huge progress achieved in the simulation of the pressure evolution. Overall, models were able to

simulate both the amplitude and the evolution tendency. The instantaneous pressure drops after the passage of the sinking face were also reproduced in some cases.

LML introduced in their model the desaturation and the coupling between damage and permeability. The model reproduces well, over a short time, the pressure drop after the passage of the sinking face. However, over long term, the pressure drop is overestimated compared to the *in-situ* case (Figure 41).

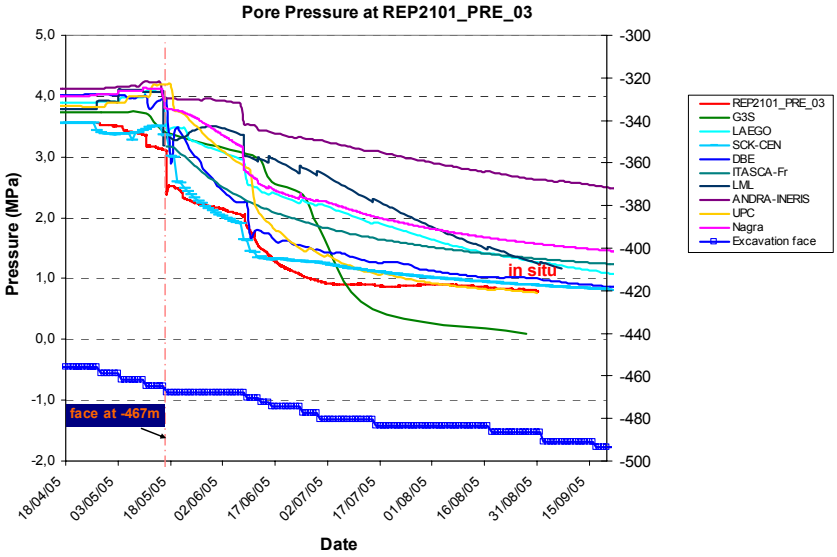

Figure 40. Comparison between measurements and interpretative models of pore pressures measured in borehole REP2101

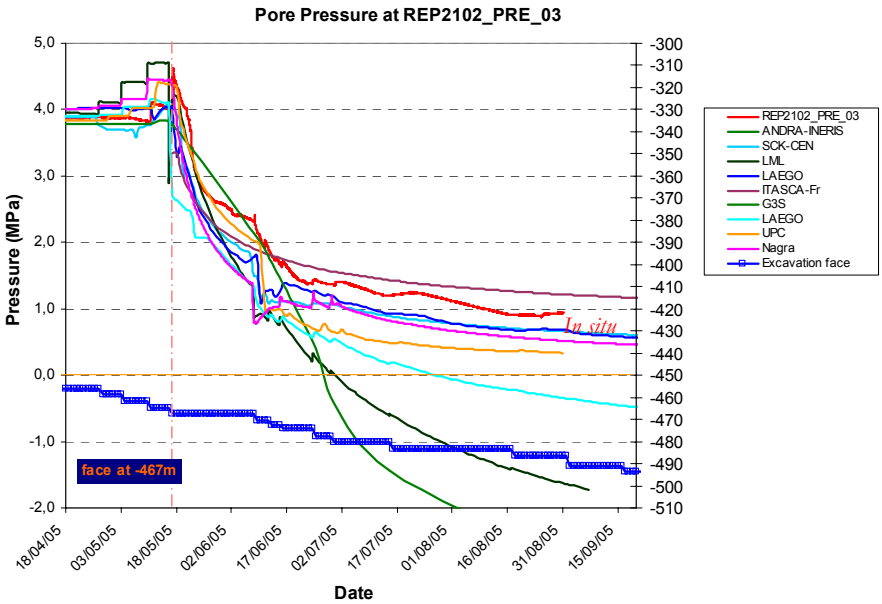

Figure 41. Comparison between measurements and interpretative models of pore pressures measured in borehole REP2102

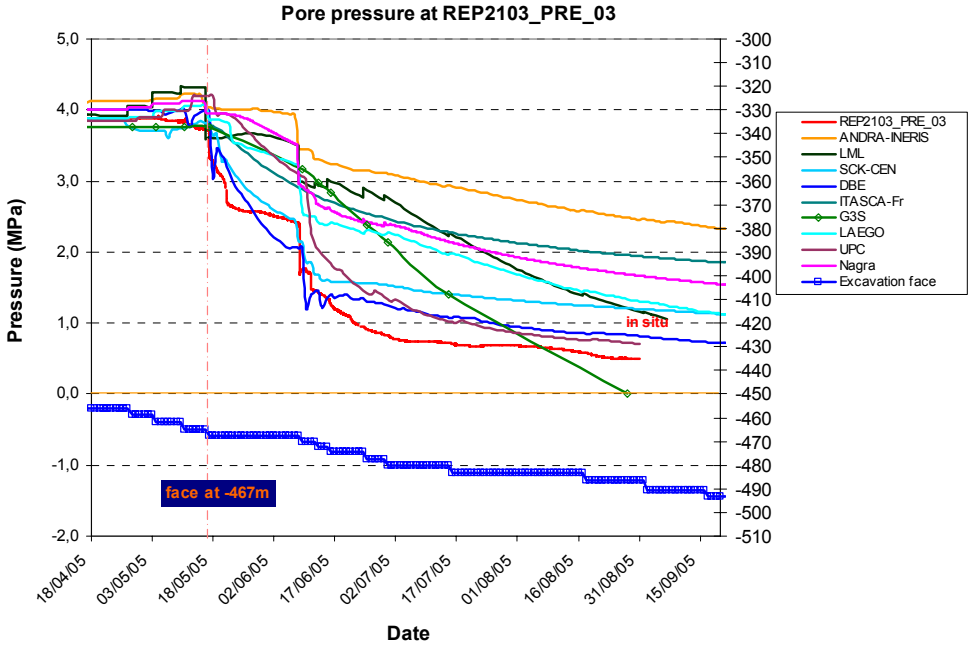

Figure 42. Comparison between measurements and interpretative models of pore pressures measured in borehole REP2103

8. CONCLUSIONS AND LESSONS LEARNT FROM THE PROJECT

8.1. Conclusions

- Gas-permeability measurements and long-term creep tests were performed on argillite samples. Original results ware obtained. The dependency of gas permeability on confining pressure is not very significant. In the testing range, the permeability perpendicular to the bedding plane is about one order of magnitude lower than that parallel to the bedding. Creep tests under variable relative humidity highlights the dominant effects of dehydration/saturation processes on time-dependent deformation mechanisms in the argillites. The anisotropy of the creep rate measured is negligible.
- The capability test of numerical codes shows that the codes used by the project are able to simulate the hydro-mechanical coupling in the rock, especially in the case of a 2-D problem with a poro-elastoplastic constitutive model.
- Based on past and new laboratory test results, both short and time-dependent behaviour models of the Callovo-Oxfordian argillites have been developed by the MODEX-REP teams. For short-term behaviour, an elastoplastic model with or without softening or hardening, an elastoplastic model with damage, a discrete model and a hydro-mechanical coupling model were proposed for the argillites. Concerning time-dependent behaviour, various methods were used: a viscoplastic model, a differed-damage model and differed-bond failure model.
- Predictive modelling (blind prediction) of the REP experiment was conducted in two steps: the first step took place in March 2003 and was based on the scheduled excavation method and the REP-experiment design. The second predictive modelling (blind prediction) was performed between April and October 2005. In general, numerical models tended to overestimate shaft convergence. Numerical results concerning the pore-pressure evolution of the measurement points were very scattered. Only a few teams provided a relatively sound agreement with *in-situ* measurements in some measurement points. While the desiccation phenomena and the change of permeability in the EDZ were taken into account in models, the results reproduced approximately the pressure evolution in some points. The displacements supplied by the different teams remain very scattered.
- By analysing the gaps between numerical and *in-situ* measurements, orientations for improving numerical and constitutive models for the argillites were discussed. In addition, in order to make future comparisons, the reliability of the precision of *in-situ* measurements was graded according to the analysis of all parameters involved in the instrumentation set-up. The interpretative modelling carried out between October 2005 and February 2006 shows the significant progress achieved. The gaps between numerical and *in-situ* measurements were significantly reduced.

In order to show the advancement made between blind prediction and interpretative modelling, Table 9 proposes a general note for the numerical modelling with regard to four aspects: shaft convergence, displacement, pore-pressure evolution and EDZ extension.

Table 9. General note for the results of the comparison between numerical models and in-situ measurements

Global note		
	Blind prediction	Interpretative modelling
Convergence	2.5	3
Displacement in rock mass	2	3
Pore-pressure	2	3
EDZ (extension)	3	3

4: very good: the phenomena are correctly reproduced both their evolution over time and their amplitude
3: good: the phenomena are reproduced over time, but their amplitude is significantly different
2: passable: the phenomena are reproduced approximately over time, but their amplitude is total different
1: not good: neither evolution and amplitude were reproduced

8.2. Lessons learnt

- The scale effect on the strength of the argillites located in the REP section is small due to the high homogeneity of the rock in that zone. Based on the damage and failure criteria determined by the average value of laboratory-test results, it was possible to reproduce the EDZ extension.
- The extension of the very limited fractured zone and of the microfractured zone was correctly forecasted by numerical models. From that point of view, the capability of models for predicting the EDZ extension is good in the case of the argillites located in the section of REP experiment.
- The short-term constitutive models for the argillites at low and medium deviatoric-stress levels need to be improved in order to understand the instantaneous water-pressure drop and the pressure distribution in the near-field as observed during the REP experiment. The effect of ventilation on water pressure within the adjacent rock mass requires further investigations.
- The capability to forecast (blind prediction) the hydro-mechanical coupling of argillites must be improved. The issue about the failure and damage criteria of argillites using effective stress is still pending. It is particularly important for assessing the time-dependent behaviour of argillites through hydro-mechanical calculations.

In conclusion, the MODEX-REP project has shown that the blind prediction of *in-situ* experiments remains an efficient way to assess the capability of numerical models and constitutive laws to simulate the evolution of underground structures over time.

9. DISSEMINATION AND USE OF RESULTS

9.1. Use of MODEX-REP results in technical reports

No	Title	Organisation	Results used
CRPADS04.0022	*Référentiel du site de Meuse/Haute-Marne*	Andra	Constitutive models
DNT1INE05025	*Modélisation 3-D du creusement des galeries expérimentales à – 490 m*	Andra-INERIS	Constitutive models
DRPADPE050855	*Résultats des mesures après la phase de fonçage du puits entre les cotes – 454 et – 480 m expérimentation REP*	Andra	Blind prediction
CNTASMG02068	*Modélisation des perturbations mécaniques et thermomécaniques autour des ouvrages dans les argillites du Callovo-Oxfordien*	Andra	Constitutive models
CNTASMG05008	*Modèle élastoplastique avec écrouissage pour les argillites développé dans le cadre du projet MODEX-REP – Mise à jour des paramètres*	Andra	Constitutive models

9.2. Deliverables

[1] 2002. Analysis of the capacity of numerical models to simulate excavation in deep argillaceous rock, compiled by K. Su. Deliverable of the MODEX-REP project, FIKW-CT2000-00029.

[2] 2002. Experimental study of the hydro-mechanical behaviour of the Callovo-Oxfordian argillites, ZHANG CL., DITTRICH J., MULLER J., ROTHFUCHS T., Deliverable of the MODEX-REP project, FIKW-CT-2000-00029.

[3] 2003. Constitutive Models of the Meuse/Haute-Marne Argillites, compiled by K. Su. Deliverable of the MODEX-REP, FIKW-CT2000-00029.

[4] 2006. Hydro-mechanical modelling of the argillites response to shaft sinking, compiled by K. Su. Deliverable of the MODEX-REP, FIKW-CT2000-00029

9.3. PhD theses concerning the modelling of the REP experiment in the MODEX-REP project

[1] Miehe B (2004): Modélisation de la zone endommagée induite par le creusement du puis d'accès au laboratoire souterraine de Meuse/Haute-Marne (argilite de l'Est). Thèse de l'Ecole des Mines de Paris, soutenue le 14 mai 2004

[2] Jia Y. (2006): Contribution à la modélisation thermo-hydro-mécanique des roches partiellement saturées – application au stockage des déchets radioactifs. Thèse de l'Université de Lille I, soutenue le 06 juillet 2006

[3] Maiolino Siegfried (2006): Réponse à l'excavation d'un massif rocheux. Thèse de l'Ecole Polytechnique, soutenue le 7 avril 2006

9.4. Publications

[1] Ferreri R., Su K., Tijani M. (2001) Développement des modèles hydromécaniques couplés dans les argilites du Callovo-Oxfordien – Résultats de la première année de MODEX-REP. Bilan des études et travaux de l'Andra 2001, 119-124.

[2] Su K., Shao J-F, Dedecker F. (2002) Modèle de comportement court et long terme des argilites de Meuse/Haute-Marne – Résultats de la deuxième année du projet européen MODEX-REP. Bilan des études et travaux de l'Andra 2002, 94-98.

[3] Su K. (2003) Development of hydro-mechanical constitutive models for Callovo-Oxfordien argillites : The MODEX-REP project. Proceedings of a European Commission CLUSTER conference, 242- 247, Luxembourg, November 2003.

[4] Su K. (2006) Synthesis of results from European MODEX-REP project. Workshop organised by Andra 21-23rd Jun 2006 at Meuse/Haute-Marne underground research laboratory.

[5] Souley M., K. Su, M. Ghoreychi and G. Armand (2003) – "Constitutive models for rock mass : numerical implementation, verification and validation" in *FLAC and Numerical Modeling in Geomechanics,* Brummer et al. (eds), 2003 Swets & Zeitlinger B.V., Lisse, ISBN 90 5809 581 9, pp. 71-80

[6] Shao J.F., Zhu Q.Z, Su K. (2003) Description of Creep in Rock Materials in Termes of Mmaterial Degradation, Computer & Geotechnics 30, 549-555.

[7] Y. Jia, X.C. Song, G. Duveau, K. Su, and J.F. Shao (2006) Elastoplastic damage modelling of argillite in partially saturated condition and application, Clay in Natural & Engineered Barriers for Radioactive Waste Confinement. Part 2, Physics and Chemistry of the Earth, Volume 32, Issues 8-14, pages 656-666.

[8] Su K. (2003) Development of hydro-mechanical constitutive models for Callovo-Oxfordien argillites: The MODEX-REP project. Proceedings of a European Commission CLUSTER conference, 242- 247, Luxembourg, November 2003

10. REFERENCES

[1] MODEX-REP, FIKW-CT2000-00029 – Deliverable 1 – *Analysis of the capacity of numerical models to simulate excavation in deep argillaceous rock* – compiled by K. Su

[2] ZHANG CL., DITTRICH J., MULLER J., ROTHFUCHS T. – *Experimental study of the hydro-mechanical behaviour of the Callovo-Oxfordian argillites* – Deliverable N° 4 of the MODEX-REP project – FIKW-CT-2000-00029, 2002

[3] MODEX-REP – FIKW-CT2000-00029 – Deliverable 2 & 3 – *Constitutive Models of the Meuse/Haute-Marne Argillites* – compiled by K. Su

[4] Su K. (2002) Specification of predictive modelling of the REP experiment. Andra Report n° C SP ASMG 02- 055

[5] Su K. (2005) Specification for modelling of the REP experiment (2005). Andra Report n° C SP ASMG 05-0024

[6] Volckaert G., Bernier F., Sillen X., Van Geet M., Mayor J., Göbel I., Blümling P., Su K.(2004) Similarities and Differences in the Behaviour of Plastic and Indurated Clays. Euradwaste 2004

[7] Hoteit N., Ozanam O., Su K., François O., Heitz J.F., Nguyen Minh D. (1999) Gomechanical research for radwaste disposal in deep clays - first results and prospects. TUCSON 2000

[8] Chiarelli A.S. (2000) Etude expérimentale et modélisation du comportement mécanique des argilites de l'Est – influence de la profondeur et de la teneur en eau. Thèse de l'Université des Sciences et Techniques de Lille

[9] Andra (2005) Dossier 2005 – Référentiel du site de Meuse/Haute-Marne. C.RP.ADS.04.0022.B

[10] Ramambasoa N. (2001). Etude du comportement hydromécaniquedes argilites – Application au site de Tournemire. Thèse de l'Ecole polytechnique. Janvier 2001

[11] Armand G., Su K. (2005) Expérimentation REP – Résultats des mesures après la phase de fonçage du puits entre les cotes - 454 et - 480 m. Rapport Andra n° DRPADPE05.0855

Contact details concerning follow-up of the MODEX-REP project

Official participants

Company	Contact person	Address
Agence nationale pour la gestion des déchets radioactifs (Andra)	Kun Su	DS/MG 1-7 rue Jean-Monnet F-92298 Châtenay-Malabry Kun.Su@andra.fr
Coyne et Bellier	Anne Bouvard	9, allée des Barbanniers F-92632 Gennevilliers Anne.Bouvard@coyne-et-bellier.fr
Empresa nacional de residuos radiactivos, SA (ENRESA)	Juan Carlos Mayor	Emilio Vargas 7 E-28043 Madrid jmaz@enresa.es
Gesellshaft für Anlagen-und Reaktorsicherheit (GRS)	Rothfuchs Tilmann	Final Repository Safety Research Division Theodor-Heuss-Strasse 4 D-38122 Braunschweig ROT@grs.de
Nationale Genossenshaft für die Lagerung radioactiver Abfälle (Nagra)	Peter Blu	Hardstr. 73 CH-5430 Wettingen blumling@nagra.ch
Belgian Nuclear Research Centre (SCK/CEN)	Sillen Xavier	Waste & Disposal Dept. Boeretang 200 B-2400 Mol xsillen@SCKCEN.BE
Groupement d'intérêt public pour l'étude des structures souterraines de stockage	Nguyen Minh Duc	G3S-LMS École polytechnique F-91128 Palaiseau Cedex duc@lms.polytechnique.fr
Université des sciences et technologie de Lille, Laboratoire de Mécanique de Lille	Jian-Fu Shao	LML Université de Lille Cité scientifique F-59655 Villeneuve d'Ascq Jian-Fu.Shao@polytech-lille.fr
École nationale supérieure des mines de Paris	Michel Tijani	CGES 35, rue Saint Honoré F-77305 Fontainebleau Cedex tijani@cges.ensmp.fr
ITASCA Consultants SA	Daniel Billaux	ITASCA Consultants SA 64, chemin des Mouilles F-69130 Ecully d.billaux@itasca.fr

Centro internacional de métodos numericos en la enginería (CIMNE)	Antonio Gens	Gran Capitan s/n – Edificio C1 Campus Norte – UPC E-08034 Barcelona Antonio.Gens@upc.es

Participants invited by Andra for some tasks and progress meetings

Company	Contact person	Address
Laboratoire Environnement, géomécanique et ouvrages (LAEGO)	Richard Giot	Rue du doyen Marcel Roubault BP 40 F-54501 Vandoeuvre-lès-Nancy richard.giot@ensg.inpl-nancy.fr
Institut national de l'environnement industriel et des risques (INERIS)	Mountaka Souley	École des Mines de Nancy Parc de Saurupt F-54042 Nancy Cedex Mountaka.SOULEY@ineris.fr
Deutsche Gesellschaft zum Bau und Betrieb von Endlagern für Abfallstoffe mbH (DBE	Michael Jobmann	DBE Technology GmbH Postfach 11 69 D-31201 Peine jobmann@dbe.de
Kungliga tekniska högskolan (KTH)	Oven Stephansson	S-100 44 Stockholm ove@gfz-potsdam.de
Electricité de France (EDF)	Patrick Desgree	Route de Sens Ecuelles F-77250 Moret-sur-Loing patrick.desgree@edfgdf.fr